A FOUNDATIONAL STUDY OF A NEW SYNTHETIC METHOD OF METAL CARBONYL CLUSTERS

by

Miles Shaun Millard

A thesis

submitted in partial fulfillment

of the requirements for the degree of

Master of Science in Chemistry

Boise State University

August 2019

BOISE STATE UNIVERSITY GRADUATE COLLEGE

DEFENSE COMMITTEE AND FINAL READING APPROVALS

of the thesis submitted by

Miles Shaun Millard

Thesis Title: A Foundational Study of a New Synthetic Method of Metal Carbonyl Clusters

Date of Final Oral Examination: 08 May 2019

The following individuals read and discussed the thesis submitted by student Miles Shaun Millard, and they evaluated his presentation and response to questions during the final oral examination. They found that the student passed the final oral examination.

Adam C. Colson, Ph.D.	Chair, Supervisory Committee
Eric Brown, Ph.D.	Member, Supervisory Committee
Michael P. Callahan, Ph.D.	Member, Supervisory Committee

The final reading approval of the thesis was granted by Adam C. Colson, Ph.D., Chair of the Supervisory Committee. The thesis was approved by the Graduate College.

DEDICATION

I dedicate this thesis to my parents who I am sure are just as excited to see me finish school as I am.

ACKNOWLEDGEMENTS

I would like to thank my advisor, Adam Colson Ph.D., for the help and guidance throughout the entire process of my Masters. I enjoyed learning from him and working in his laboratory. He made the process seem more manageable and at times fun. I would also like to thank Joseph Dumais Ph.D. for all of his help and patience in running a multitude of NMR experiments. A big thank you to the rest of my committee Eric Brown Ph.D. and Michael Callahan Ph.D. Finally, thank you to the faculty of the Boise State University Department of Biochemistry and Chemistry for letting me learn from you for the past three years. Thank you.

ABSTRACT

"Traditional" Metal Carbonyl Clusters (MCCs) contain a framework of multiple metal atoms bound together through formal metal-metal (M-M) bonds. Current methods of synthesis result in different cluster sizes and lack a method to control growth. This project proposes a new method of MCC synthesis to build larger structures utilizing secondary non-covalent interactions to develop "non-traditional" MCCs. The *N,N'*-diarylurea moiety is a strong hydrogen bond donor/acceptor that can induce self-assembly into larger secondary structures. The union of metal carbonyl and urea chemistry provides a potential method of "non-traditional" MCC synthesis. This proof of concept experiment will elucidate foundational information such as: reduction-oxidation potentials, chemical organization, chemical structure, and binding constants. The x-ray crystal structures detail a nearly planar molecular organization and refute the formation of urea ribbons due to a stabilizing intramolecular hydrogen bond interaction. Stabilizing π-π stacking and a urea-π stacking interactions were observed as a result of the planar orientation. A titration study confirms the strong anion binding capability of the metal carbonyl appended urea moiety and confirms anion binding as a possible method of coordinating multiple units together to build "non-traditional" MCCs. The π-π interactions and urea-π interactions were observed as the largest contributor to the molecular structure and as a result, the appended group 6 metal centers are separated by distances between 6.00 Å and 8.00 Å. The close contact between metal nuclei has the potential to allow for electrochemical communication albeit not with these compounds. The characterization and synthesis of 1,3-bis(p-

isocyanophenyl)urea and its group 6 metal containing derivatives provided sufficient data to lay a solid foundation for continuing research.

TABLE OF CONTENTS

LIST OF TABLES

LIST OF FIGURES

LIST OF ABBREVIATIONS

MCC	Metal Carbonyl Cluster
CO	Carbonyl
NC	Isocyanide
NMR	Nuclear Magnetic Resonance

CHAPTER ONE: BACKGROUND

1.1 Introduction to Metal Carbonyl Cluster Chemistry

The transition metals are of interest to many because there is still a lot of chemistry to be discovered. One area of interest that has been around since the 1930s is metal carbonyl cluster (MCC) chemistry.[1,2] Due to the increase of electron density of the transition metals, the nuclei are bound to ligands such as carbon monoxide (CO) that stabilize the electron rich nuclei as shown in Figure 1a. MCCs are multinuclear compounds containing a framework of metal atoms bound together through formal metal-metal (M-M) bonds as shown in Figure 1b. The first metal carbonyl compounds were discovered between the 1930s and the 1950s in the form of $Co_2(CO)_8$, $Fe_2(CO)_9$, and $Fe_3(CO)_{12}$.[1,2] MCCs can vary in size depending on the synthetic method used and there is some debate on the minimal amount of metal centers required to be defined as a cluster; however, that number is subjective and speculative. Traditionally, three metal nuclei is the most common minimal amount required to be considered a cluster.[3] MCCs were the subject of many studies during the 1970s and 1980s because of promising results in catalysis, the cluster cores acting as electron reservoirs, and nanoparticle development.[3,4] For a cluster to be considered an electron reservoir it must be able to undergo reversible reduction and oxidation events. Figure 2 shows an example of a CO stabilized cluster that exhibits the electron reservoir

property. When exposed to an electric potential, the $[Ni_{32}C_6(CO)_{36}]^{6-}$ complex shows the ability to accept and donate electrons as depicted in Figure 2b.

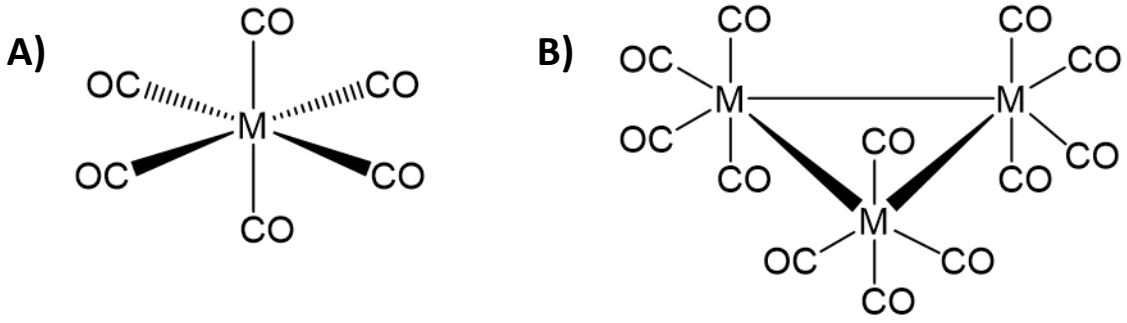

Figure 1 A)Example of a generic saturated metal carbonyl, B) Example of a generic saturated metal carbonyl cluster.

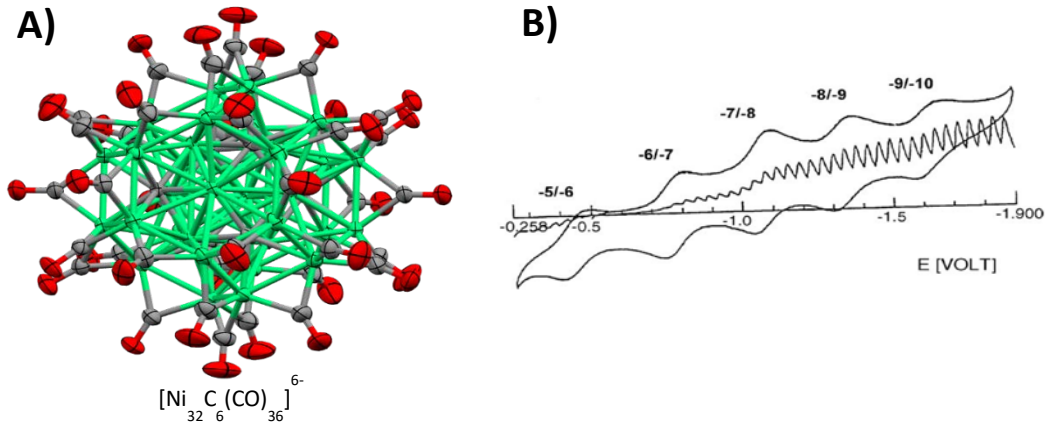

Figure 2 A) Model metal carbonyl cluster depicting 32 metal centers, 6 interstitial carbons, and 36 CO stabilizing ligands. B) The oxidation-reduction potential of the $[Ni_{32}C_6(CO)_{36}]^{6-}$ MCC.

1.2 The Traditional Synthetic Methods of MCCs

Coordinatively saturated metal species are relatively unreactive but coordinatively unsaturated metal species are able to condense into larger clusters. Traditionally, these clusters have been designed using three well-documented synthetic pathways: photolysis, pyrolysis, and chemically induced condensation reactions. [1,5] While these methods are proven, they are not methods to synthesize predefined structures; rather they are methods to promote growth. An example of this growth is shown in Figure 3 by the condensation

of $Os_3(CO)_{12}$, by pyrolysis to yield: $Os_5(CO)_{16}$, $Os_6(CO)_{18}$, $Os_7(CO)_{21}$, and $Os_8(CO)_{23}$.[5,6] Even though these methods of synthesis are effective, the product distribution is very broad. This project proposes a new method of MCC synthesis that will allow for some control over the product distribution. One possible method of synthesis is to build larger structures via self-assembly through secondary non-covalent interactions to develop "non-

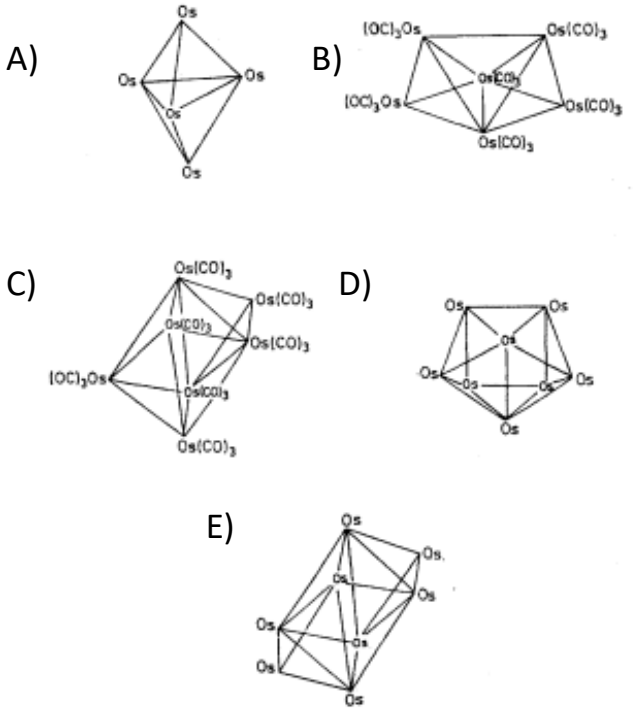

Figure 3 Possible metal carbonyl cluster geometries A. $Os_5(CO)_{16}$, B. $Os_6(CO)_{18}$, C. $Os_7(CO)_{21}$, D. $Os_8(CO)_{23}$ and E. $Os_8(CO)_{23}$

traditional" metal carbonyl clusters.

A "traditional" MCC might be more simply defined as a complex with multiple metal nuclei upon further deconstruction. A structure that contains at least three metal nuclei but that are not covalently bound may still fall under the simple definition of a MCC but labeled as a "non-traditional" MCC. As long as there are multiple metal centers available it might be conceivable that the properties "non-traditional" MCC to resemble a "traditional" MCC.

1.3 Introduction to the Diaryl Urea Moiety

The urea moiety is ubiquitous throughout chemistry and biology and has been the subject of many discussions.[7–9] Recently, urea has been exploited for its use in building larger secondary structures via self-assembly.[7] Several key features of the urea moiety give it the unique ability to self-assemble into larger structures. First, the carbonyl of the urea is a powerful hydrogen bond acceptor and the hydrogens on the urea nitrogens are strong hydrogen bond donors. The hydrogen bonding capability of the urea moiety allow for self-association into foldamer structures and hydrogen-bonded chains as seen in Figure 4a.[7,10–12] Second, the strong hydrogen bond donor ability of the urea hydrogens also allows for binding around various anions and opens up the possibility of using urea as a templating agent as seen in Figure 4b.[13]

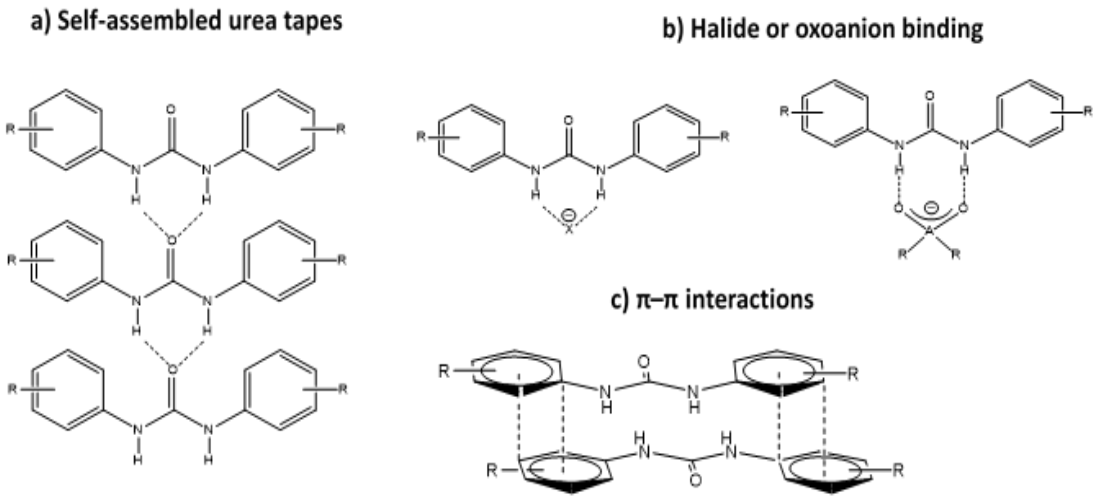

Figure 4 Various modes of self-assembly of the urea moiety. a) Urea tapes facilitated by strong hydrogen acceptor-donor ability of the urea carbonyl and urea N-Hs b) Anion complexes possible due to the hydrogen bond donor ability of the urea N-Hs c) Stabilizing π- π interactions

From Figure 4b it is easy to see how one urea moiety would attract one anion in a 1:1 ratio. However, depending on the strength of the urea binding pocket (*host*) and the strength of the anion (*guest*) different ratios of binding can occur other than a simple 1:1

ratio. The other ratios that could be seen, 1:2 or 1:3, stem from increasing the number of urea functional groups in the host molecule which would allow for multiple anion molecules to be bound.[14] Additionally, the crystal packing organization might also be affected by the binding strength of the urea moiety.

Crystal engineering can be impacted by anion binding through co-crystallization with the anions which can affect the overall crystal packing and physical properties.[15,16] Co-crystallization with a cation/anion pair will cause the spatial orientation in the crystal lattice structure to be altered in some manner. A potential change in crystal packing could be facilitated by strongly basic anions because the strongest hydrogen bonds are formed by the most electronegative anions.[40] Anion binding will play a large roll in crystal engineering and in finding ways to alter the crystal packing structure. As previously mentioned, MCCs are characterized by their electronic properties which are typically examined in the solid state and being able to modify the solid crystal structure will aide in further experimentation. Finally, the urea moiety can be further functionalized with aryl rings on either side to promote self-assembly into larger structures via π-stacking interactions.[17–19]

There are several parameters that affect the stabilizing π-stacking interactions. First, most of the information will be gathered in the solid state because the molecules will be locked in a conformation. In the liquid state the urea moiety will rotate and spin on an axis disrupting the π-stacking interactions. Secondly, the distances between molecules will determine if the stabilizing effect is actually a result of π-stacking. The normal range for π-stacking distances is between 3.3 – 3.8 Å. Finally, there are several ways that π-stacking aromatic rings can arrange: parallel stacked, offset stacked, or T-shaped. Depending on

other steric interactions or potential solvent interactions one of those arrangements will be preferred.[17,18] Understanding the fundamental elements surrounding the *N,N'*-diarylurea moiety is vital in trying to develop a "non-traditional" style of MCC.

This project will detail the union of metal carbonyl and urea chemistry by examining the various intermolecular interactions observed in the functionalized *N,N'*-diarylurea moiety appended to group 6 metal carbonyls and lay the foundation for methods of synthesis for non-traditional MCCs.

1.4 Introduction to Carbonyl (CO) and Isocyanide (NC)

As previously stated, CO ligands surround transition metals to form stable complexes.[20] The CO ligand is able to achieve the stabilizing effect because of its unique molecular orbitals. CO's molecular orbitals are shaped such that the filled σ-orbital lies on the carbon molecule and the empty two π^*-orbitals also reside on the carbon molecule. Electron rich metal centers can be stabilized by offloading, or back donating, electrons into the empty π^* orbitals. This orbital configuration, shown in Figure 5a and Figure 5c, is what makes CO considered to be a weak σ-donor and a stronger π-acceptor.[20] The isocyanide ligand (NC) has a similar molecular orbital to CO as seen in Figure 5b and 5d and as a result exhibits similar sigma-donor and π-acceptor properties.[20,21]

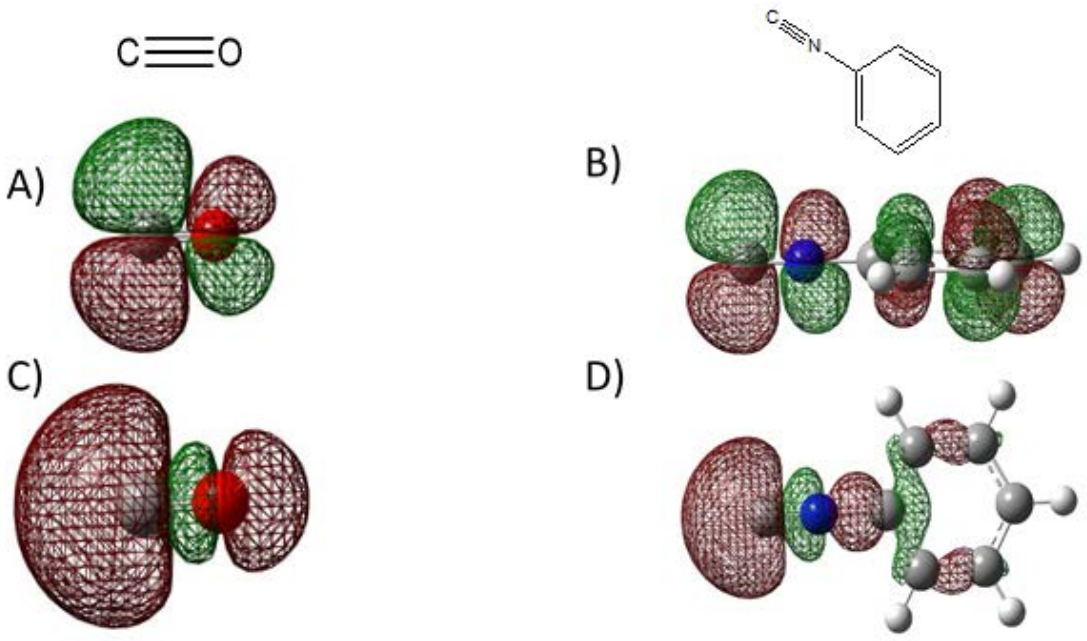

Figure 5 (A) Molecular model of CO σ-orbital (B) Molecular model of aryl isocyanide σ-orbital (C) Molecular model of CO π^*-orbital (D) Molecular model of aryl isocyanide π^*-orbital

A ligand can be identified as a π-accepting ligand by evaluating bond distances from the metal center to the ligand. Strong π-acceptors, such as CO, see a shortening M-C bond length but a lengthening of the C-O bond as depicted in Figure 6. The lengthening of the C-O bond is a result of the electron rich metal center offloading electrons into the CO ligand π * -orbitals. As the π * -orbitals (antibonding) are populated the bond order decreases and is observed by the increase in distance between the C-O. Experimental evidence documents the NC ligand as a π-acceptor, but not as strong as CO.[22,23] These similarities in bonding properties are attributed to the isolobal structures of molecular orbitals of CO and NC. Furthermore, unlike the CO ligand, the NC ligand has been shown to be functionalized in other organic molecules which would allow for the incorporation of other stabilizing groups such as an aryl ring.[20]

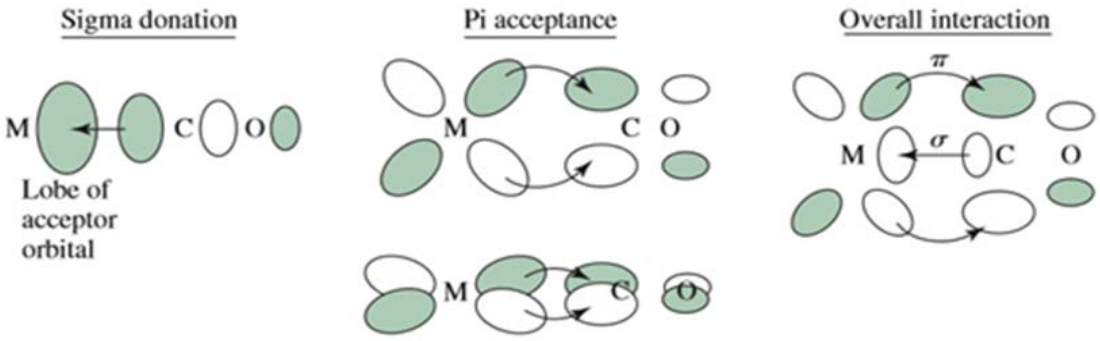

Figure 6 σ-donor and π-acceptor diagram of a metal with a CO ligand

1.5 Union of Urea Chemistry and MCC Chemistry: A New Synthetic Method of Non-traditional Clusters

My research hypothesis asks if the self-assembly/templating characteristics of the urea moiety can be utilized in bringing multiple metal carbonyls into close contact in order to elucidate previously unknown structural organizations. There are multiple accounts of the urea moiety forming larger secondary structures via non-covalent interactions as well as the NC ligand being further functionalized after attachment to a metal.[7,24,25] With all the potential applications of MCCs and the lack of continual research, the field is prime for a new synthetic method to emerge that allows for advancements and rejuvenation of the MCC era. Due to this project being a proof of concept experiment, a lot of the work surrounding the synthesized compounds will be to determine foundational information such as: reduction-oxidation potential, chemical organization, chemical structure, and binding constants. Finally, this thesis will take a brief look into future avenues of interest that will be available as a result of this fundamental research.

CHAPTER TWO: SYNTHESIS, CHARACTERIZATION, AND PROPERTIES OF METAL APPENDED *N*,*N*'-DIARYLUREAS

2.1 Introduction

Metal carbonyls are transition metals that are stabilized by the carbon monoxide (CO) ligand. The CO ligand allows for the electron rich metal center to off-load electron density to the empty π^*-orbitals of the CO, thus stabilizing the compound.[1,26] A conglomeration of metal carbonyls will yield a metal carbonyl cluster (MCC). Low-valent metal clusters have been of interest since the early 1970s due to their connection to nanoparticles and nanotechnology. Initial studies explored applications as electron reservoirs and homogeneous catalysts, but it was determined that cluster fragments of the overall larger cluster were responsible for these properties.[4] Further studies have suggested that several reported metal carbonyl clusters share properties similar to nanocapacitors. [4,27] A major road block in the advancement of MCC chemistry is the large product distribution. The traditional methods of synthesis rely on thermal, photochemical, or redox condensation to build larger and larger structures, but because these methods rely on unsaturated metal nuclei reacting with one another, the range of products varies. This remains the largest barrier to the advancement of MCC chemistry.[1,5]

It is hypothesized that larger MCC subunits can be designed through incorporation of organic ligands capable of non-covalent interactions that promote self-assembly as shown in Figure 7. Through the incorporation of a linker molecule capable of non-covalent interactions it should be possible to assemble a larger structure that incorporates metal

carbonyls. An integral part of supramolecular chemistry is determining the method that promotes most efficient building, and the non-covalent interactions are a large contributor. As a result of the result of research in non-covalent interactions, there have been many advancements in chemical sensing, molecular recognition, and self-assembly.[28–30] In order to facilitate self-assembly, an ideal ligand would be the urea moiety which is a well-known self-assembling agent and potentially offers another way of MCC formation. [12,31,32] *N,N'*-diarylurea molecules have been examined and shown to exhibit self-assembly characteristics through non-covalent interactions such as π-stacking and hydrogen bonding to make larger secondary structures. The versatility of the *N,N'*-diarylurea moiety in promoting supramolecular interactions was the reason for its selection.[7,31] The union of

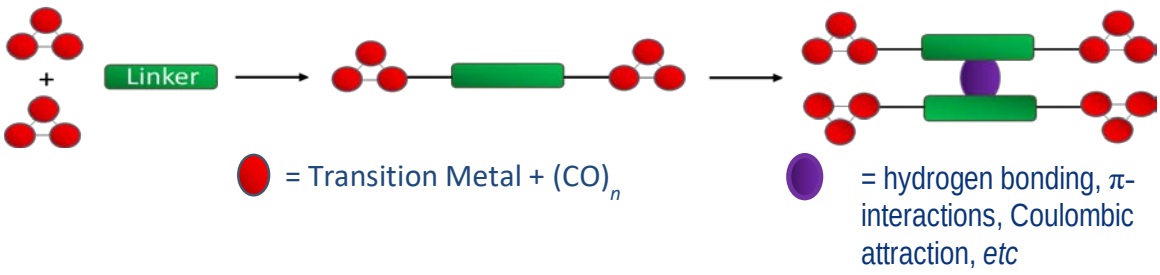

Figure 7 Generic outline of a linker molecule being attached to transition metal carbonyl and being assembly into a larger structure via secondary non-covalent interactions.

N,N'-diarylurea molecules and metal carbonyls has the potential to produce a new form of MCCs.

Conjoining a saturated metal carbonyl to a *N,N'*-diarylurea moiety is unique synthetic challenge because a CO ligand needs to be displaced and replaced with a ligand that can be further functionalized. The stabilizing CO ligand is a strong π-acceptor and similarly, the isocyanide (NC) ligand is also a strong π-acceptor albeit weaker than CO. Isocyanides have been seen in transition metal complexes which provides precedence that

the NC ligand and a CO ligand can be switched.[21,23] The NC is the linker for metal carbonyls and *N,N'*-diarylureas and should allow for exploration of the strong secondary interactions between different metal appended *N,N'*-diarylurea moieties. Scheme 1 shows the synthetic route taken to develop the linker molecule as well as appending the metal

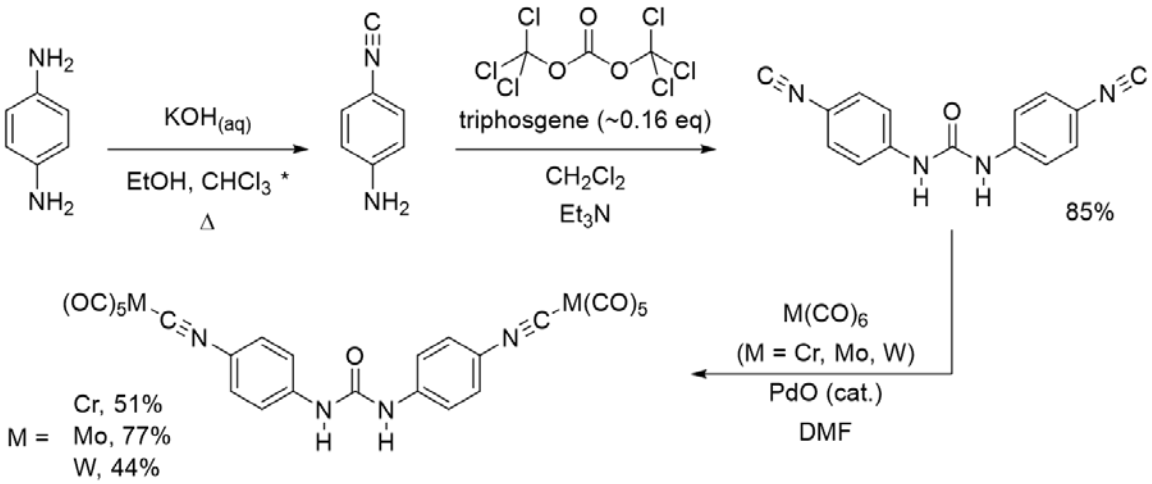

*Scheme 1: The synthetic method to create the metal appened species. * K. Heinze and J. Volker. Eur. J. Inorg. Chem.* ***2003****, 21, 3918-3923*

carbonyls. The goal is to potentially elucidated interactions between multiple metal centers that are a direct result of the organization from the *N,N'*-diarylurea non-covalent interactions to create a "non-traditional" MCC.

2.2 Results and Discussion

Table 1 shows each of the novel compounds synthesized which exclusively include 1a, 1b, 2a, 3a, 3b, and 4a. Complex 1a would include the NC substituent with the organic linker molecule labeled 'a' and complex 2b would include the $NCCr(CO)_5$ substituent and organic linker 'b' etc. Complexes 1a and 1b (**Table 1**) were both prepared by utilizing the strategy described by Heinze, and Gale to prepare a structure with similar functionalities.[33,34] Compounds 1a and 1b were purified by sublimation and solvent extraction. Compounds 2a, 3a, and 4a (**Table 1**) were prepared via chemical

decarbonylation using Trimethylamine N-oxide (TMANO) to displace a CO ligand from the metal carbonyl, $[M(CO)_6] \rightarrow [M(CO)_5]$, then an unsaturated intermediate reacts with the available carbon of the NC on compound 1b. Compound 3b (**Table 1**) was synthesized utilizing the TMANO method as well in an effort to determine as much supramolecular information as possible when only one metal was appended versus two metal centers. The NC ligand was monitored by infrared spectroscopy (IR) because the carbon did not show up well in the ^{13}C NMR and because NCs have a diagnostic peak around 2200 cm^{-1}, as summarized in **Table 1**. It is worth noting that the C≡N stretching frequency increases upon metal coordination, suggesting that the NC acts primarily as a σ-donor with very little—if any—π-accepting character. The increase in stretching frequency of the C≡N from 2127 cm^{-1} to ~2140 cm^{-1} is due to less back donation from the metal centers to the NC and is seen throughout all metal bound complexes. Alternatively, the C≡O stretching frequency decreases in all metal bound complexes suggesting that as one CO is replaced with an NC ligand, the CO ligands become better π-acceptors. The complete structures of 2a, 3a, 3b, and 4a were confirmed by single-crystal X-ray diffraction studies where the crystals were grown from an acetonitrile solution in a freezer at -20 °C.

Table 1 **Diagnostic infrared C≡N and C≡O stretching frequencies for compounds 1-4**

R = N≡C **(1)**; N≡C—Cr(CO)$_5$ **(2)**; N≡C—Mo(CO)$_5$ **(3)**; N≡C—W(CO)$_5$ **(4)**

a)

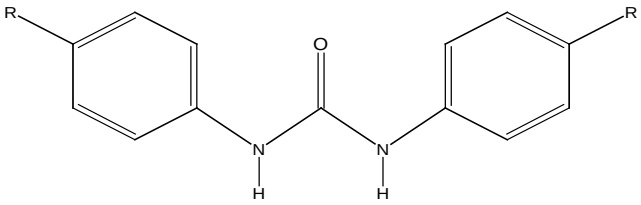

b)

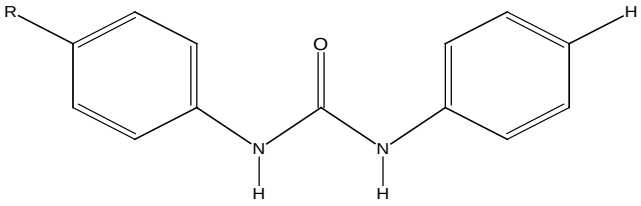

	v (N ≡ C) cm^{-1}	**v (C ≡ O) cm^{-1}**
1a	2127	N/A
2a	2143	2058, 1955
3a	2143	2063, 1956
4a	2144	2059, 1950

*Recorded in CH_2Cl_2

In order to obtain as much information supramolecular interactions, crystal structures of compounds 2a, 3a, 3b, and 4a were obtained. The crystal structures that were elucidated for compounds 2a, 3a, 3b, and 4a showed some high order packing and are shown in Figure 8 and Figure 9. Most interestingly, it was observed that complexes 2a, 3a, and 4a were essentially planar molecules as a result of the *N,N′* -diarylurea moiety intramolecular hydrogen bond interactions. It is worth noting that a different crystal organization pattern was observed for compound 3b (Figure 9a).

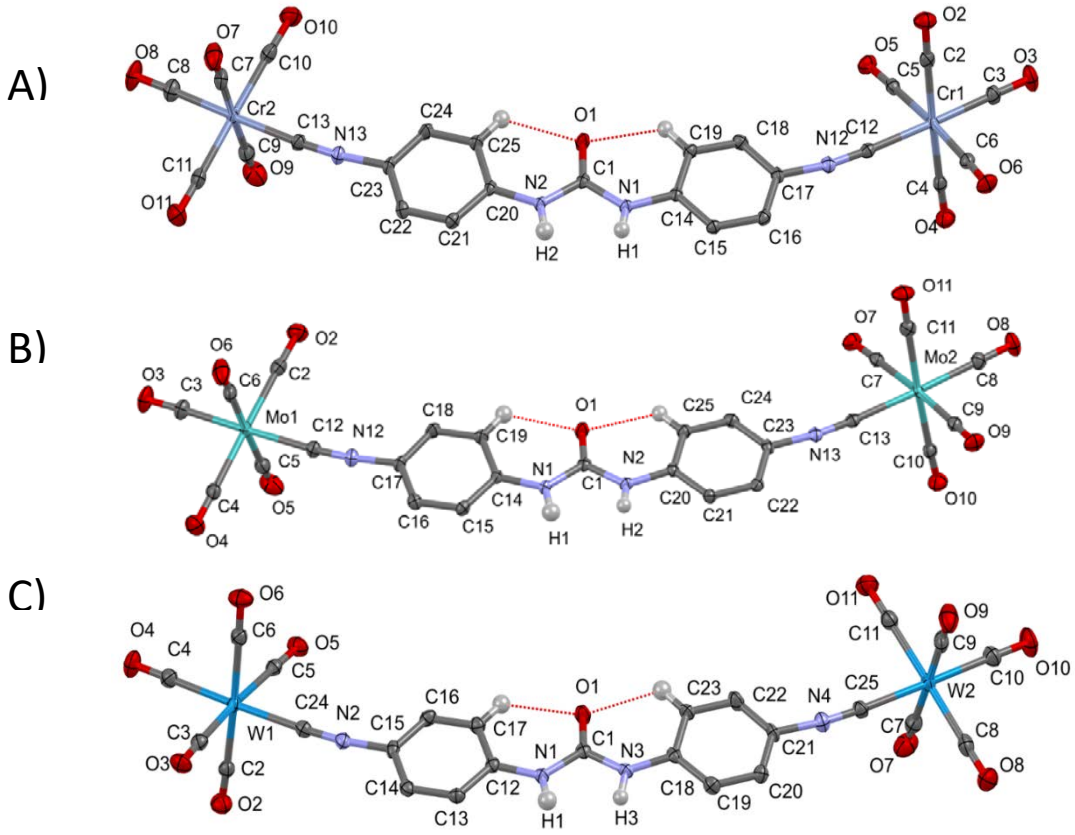

Figure 8 (A) Molecular structure of complex 2a (B) Molecular structure of complex 3a (C) Molecular structure of complex 4a. Thermal ellipsoids are rendered at the 50% probability level. Only urea N–H atoms and aromatic hydrogen atoms participating in hydrogen bonding are shown. Solvent molecules (CH_3CN) are omitted.

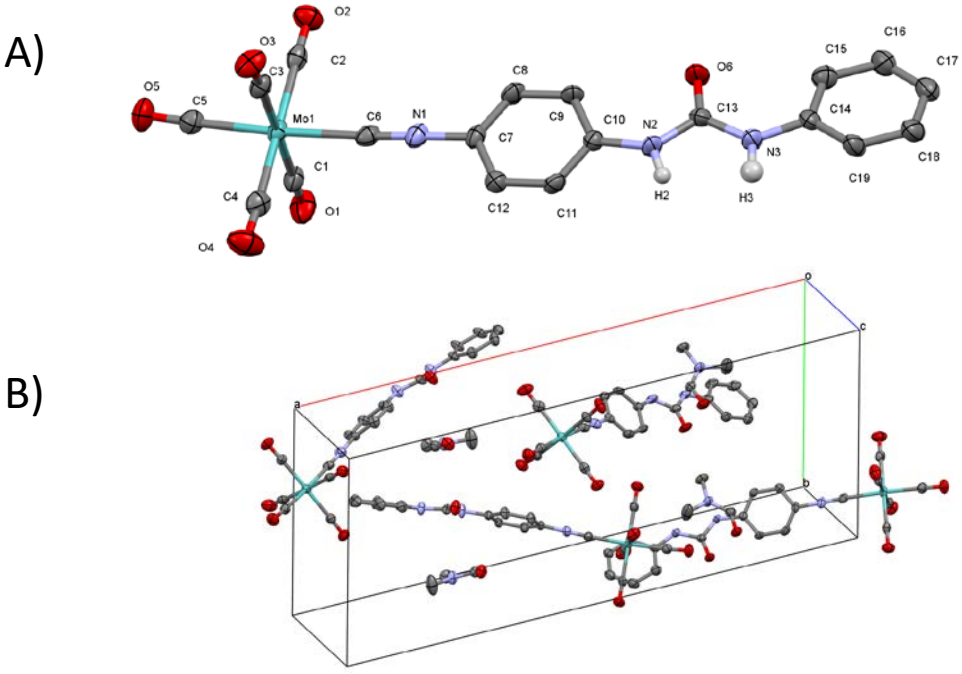

Figure 9 (A) crystal structure of complex 3b (B) Unit cell organization of complex 3b. Only urea N–H atoms participating in hydrogen bonding are shown. Solvent molecules (DMF) is shown in unit cell.

Literature examples detail how the urea moiety can form urea ribbons via hydrogen bonds as seen earlier in Figure 4. In order for the hydrogen bond interaction to occur, the phenyl ring needs to be slightly tilted out of plane from the rest of the molecule, Figure 10b. The steric hindrance between the phenyl rings is enough to disrupt the formation of the hydrogen bonds and subsequently the urea ribbons (Figure 10a).[31,36] The C_{ortho}–C_{ipso}–N_{urea}–C_{urea} torsion angles of 0.46° and 7.5° (**Table 2**) are similar to those reported by Nangia for other *N,N′*-diarylureas bearing para-substituted electron-withdrawing groups.[35]

Table 2 **Selected bond distances, close contacts, and torsion angles for complexes 2a, 3a, and 4a.**

	2a (M = Cr)	**3a** (M = Mo)	**4a** (M = W)
	Distances (Å)		
M – $C_{isocyanide}$	1.981(2), 1.979(2)	2.127(2), 2.130(2)	2.119(3), 2.113(3)
C_{ortho} – H···O_{urea}	2.24, 2.22	2.25, 2.23	2.25, 2.23
π – π ‡	3.31	3.33	3.32
urea – π ‡	3.29	3.32	3.31
	Torsion Angles (°)		
C_{ortho}–C_{ipso}–N_{urea}–C_{urea}	1.1, 6.1	0.46, 7.5	0.45, 7.8

‡ distance between adjacent mean *N,N'*-diarylurea molecular planes

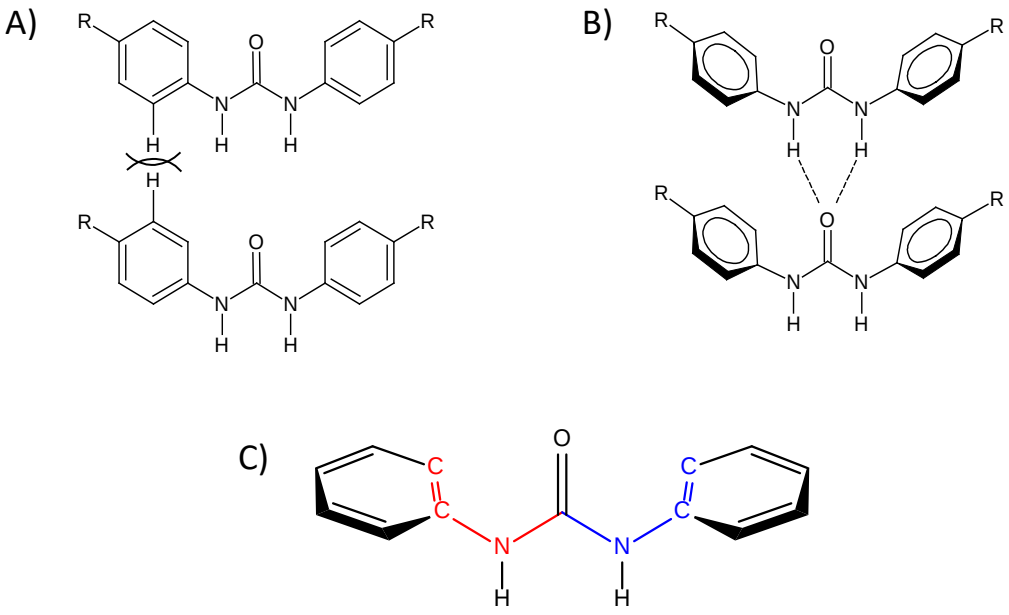

Figure 10 **(A) Planar conformation demonstrating steric interactions that prevent urea ribbon formation. (B) Absence of intramolecular hydrogen bond between ortho proton and urea oxygen that would allow for aryl ring rotation and urea ribbon formation. (C) Highlighting the atoms that are used to calculate the torsion angle and determine planarity.**

The crystal structures of 2a, 3a, and 4a clearly detail an essentailly planar orientation between the urea and the aromatic rings. Interestingly, the crystal structures do not show the formation of urea ribbons but rather show that the planar orientation is prefered due to a stabilizing intramolecular hydrogen bond interation. The planar structure is most likely attributed to an intramolecular hydrogen bond happening between the ortho aryl protons and the urea carbonyl oxygen atom showing contact distances of 2.25 Å and 2.23 Å. A similar type of arylurea intramolecular interaction was also documented by Etter.[37] Molecular modeling studies have been done that detail the *N,N'*-diphenylurea does favor the planar conformation.[18] These intramolecular hydrogen bond features are present in compounds 2a, 3a, and 4a with structural information presented in **Table 2**. The level of contribution to the molecular structure that the intramolecular hydrogen bond interaction is responsible for is visible through the torsion angles seen in **Table 2.** The planar conformation is measured by the angle of the C_{ortho}–C_{ipso}–N_{urea}–C_{urea} molecules. In complex 2a, 3a, and 4a the torsion angles are relatively similar and small and that is a direct result of the strength of the C_{ortho} – H···O_{urea} interaction. The crystal structures also show π- π interactions similar to that suggested in Figure 4 which are a large contributing factor of the prefered crystal packing. Overlapping aryl rings have been documented as a stabilizing interaction and can promote one organizational pattern over others.[18]

In the proposed π- π stacking image in Figure 4c, the aryl rings do not directly overlap but are actually staggered. This staggered pattern repeats evenly and the distances between centers of the aryl rings do not exceed 4.2 Å.[15,35] The molecular packing of compound 2a, 3a, and 4a do resemble the π-π stacking example but upon closer examination there are subtle differences. Figure 11a shows the distance between any two

molecules alternating from 3.33 Å to 3.32 Å but more importantly, the distances between the centers of the aryl rings differ from literature values. The distance from the top face of one aryl ring to the bottom face of the aryl ring above is 3.76 Å, while the distance from the bottom face of the same aryl ring to the top face of the aryl ring below is 4.79 Å. The importance of this lies within the positioning of each molecule when looking at the crystal packing from a "top-down" perspective such as in Figure 11b. Unlike Figure 4c, the stacking pattern in Figure 11a does not repeat evenly for every two molecules, instead the top and bottom face of any given molecule have different overlap patterns.

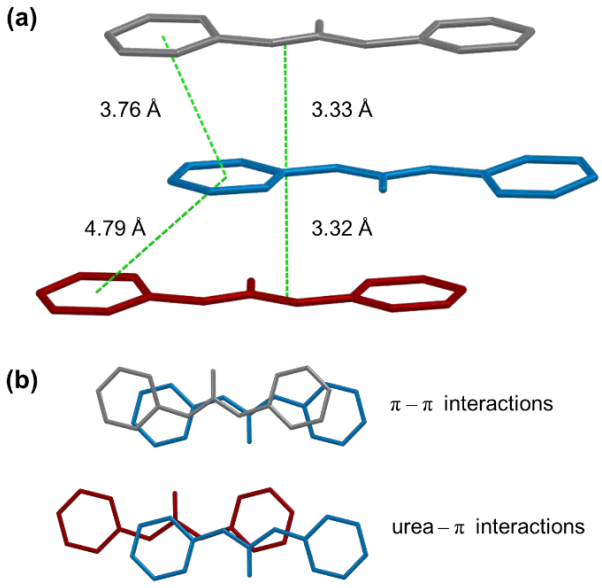

Figure 11 (a) Distances between adjacent N,N'-diarylurea planes and the aromatic ring centroids of complex 3a. (b) Alternating stacking motifs viewed normal to the N,N'diarylurea planes. Hydrogens atoms and all ring substituents are omitted for clarity

The top face interaction is most similar to a true π-π stacking interaction but the bottom face interaction is more closely related to a urea-π stacking interaction. In the latter case, the distance between the aryl ring center and the urea nitrogen atom is only 3.34 Å, suggesting the existence of a non-covalent urea–π interaction. Similar close contacts are

also observed in the Cr- and W-containing derivatives (2a and 4a), as tabulated in Table 2. Due to the planar conformation, the molecules overlapped with one another and were stabilized by π-π stacking and a urea-π stacking interaction. The crystal lattice structure of compound 3a is shown in Figure 11a and the planarity is ubiquitous even with potential steric bulk of $Mo(CO)_5$ subunits. The *N,N′* -diarylurea moiety promotes uniform packing and results in staggered placement of metal atoms (Figure 11b). The proximity of the metal atoms to one another is one of the defining characteristics of this crystal structure.

A considerable amount of interest in MCCs results in the ability of metal atoms to communicate electronically and the electron transfer process between metal nuclei. In species that are electroactive the parameter that affects electron transfer the most is physical distance. Figure 12a shows the unit cell of complex 3a and the spatial organization of multiple molecules. Interestly. in typical biological systems experience electron transfer events at a range of 4 Å to 14 Å.[38,39] With an observed separation of 6.0 to 7.6 Å between metal atoms in Figure 12b, it is easy to see potential of these compounds to evolve into a relevant charge transferring material, however, compounds 2a, 3a, 3b, and 4a are not expected to undergo reversible redox events and have only been able to undergo irreversible oxidation (Appendix-A Figure S5). It is worth nothing that the metal carbonyls appended to the organic linker molecule only have one metal nuclei, in future works if larger premade clusters were to be appended it would be expected that the crystal packing organization will be different and might not fall within the accepted distances of electronic communication.

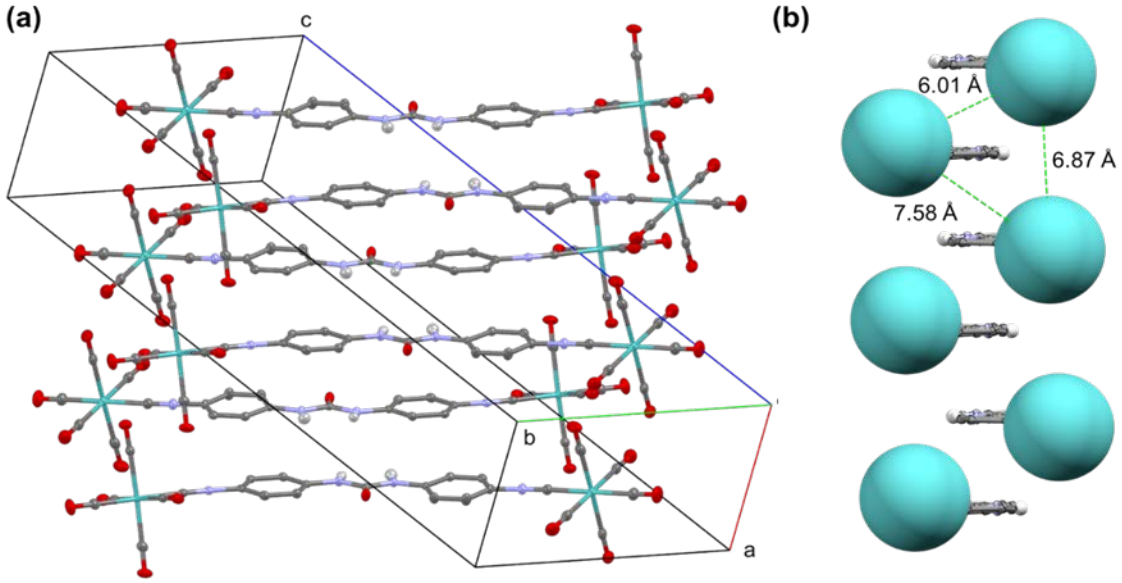

Figure 12 (a) Molecular packing of 3 with the orientation of the molecules relative to the unit cell axes shown. (b) Alternative representation of the molecular packing of 3 viewed through the N,N′ -diarylurea planes with the CO ligands omitted and Mo atoms depicted at full Van der Waals radius.

An oxidation-reduction potential of complexes 2a, 3a, and 4a was obtained in order to examine the electrochemcial properties. The cyclic voltammogram (Figure S5) shows the ability of these complexes to be irreversiblly oxidized. Interstingly these complexes undergo a two electron oxidation where one electron is removed prior to the second and at a lower potential. The electron oxidation is not surprising because the complexes have two metal centers, what is surprising is that the oxidation steps happen at different potentials suggesting that there is some intramolecular communication between the to metal nuclei. This thesis is not yet at the point to consider charge transferring materials, instead this thesis sought to identify fundamental interactions complexes 2a, 3a, 3b, and 4a to elucidate foundational chemical packing properties.

Another method to promote cluster building and crystal packing with the urea moiety is to coordinate molecules around an anion because the urea hydrogens are known

to bind anions.[7,40] A study about the anion-binding behavior in a non-aqueous solutions was carried out with compounds 1a, 1b, 2a, 3a, 3b, and 4a. The mono-urea systems typically do not self-assemble therefor the anion titration study was conducted as a foundational experiment to determine the baseline strength of anion binding.[41] All compounds were subjected to various anions to determine a baseline of binding between the urea hydrogens and different classes of anions. As representatives of the halides, inorganic oxoanions, and organic oxoanions, Cl^-, NO_3^-, and H_3CCOO^- were used in the form of their tetrabutylammonium salts. The host–guest interaction of interest can be represented by the equations in Figure 13. The interactions of host-guest chemistry can be treated as a system in equilibrium where the amount of free host (*H*) and free guest (*G*) is in balance with the complexed host-guest (*HG*). As a result of the host-guest interactions being in equilibrium, the general equilibria constant (K_a) is related to the concentrations of the [*H*], [*G*], and [*HG*]. However, only the concentrations of the [*H*] and [*G*] are known from the beginning of the experiment. Initially the concentraion of [HG] will be zero because no amount of [G] will have been titrated into the [H] solution. As the titration of [*G*] into a solution of [*H*] progresses to form the [HG] complex, there will be a change in a physical property that can be monitored, in this case chemical shift (δ) through ^{1}H NMR. The Δδ is related to the mole fraction of [HG]/$[H]_0$, monitoring the change in chemical shift at each addition of [G] to a known $[H]_0$ solution allows for the determination of the [HG]. Being able to identify the [HG] through ^{1}H NMR then enables the K_a to be determined through the use of a non-linear regression equation that requires the initial concentration of the host, $[H]_0$, the intial concentraion of the guest. $[G]_0$, and the host-guest concentraion, [HG].

A) $H + G \leftrightharpoons HG$ B) $K_a = \frac{[HG]}{[H][G]}$ C) $\Delta\delta = \delta_{\Delta HG}\left(\frac{[HG]}{[H]_0}\right)$

D) $[HG] = \frac{1}{2}\left(G_0 + H_0 + \frac{1}{\boldsymbol{K_a}}\right) - \sqrt{\left(G_0 + H_0 + \frac{1}{\boldsymbol{K_a}}\right)^2 + 4[H_0][G_0]}$

Figure 13 Equations to determine non-linear bonding constants for host-guest chemistry

A series of ^{1}H NMR incremental titrations were conducted to extract the binding constants of each anion with each new compound. All methods and calculations were set up analogous to the methods described by Pall Thordarson.[42,43] A steady increase in magnitude of binding is seen in Figure 14 with changing anions, NO_3^- < Cl^- < H_3CCOO^-, this is consistent with the literature by Bregovic et. al. As preiviously mentioned, the mono-urea host molecules were not expected to bind in any other ratio than 1:1 and that is what was observed in the mass spectrometry data in Appendix A. In Figure 14, the two separate linear portions of the graph will intersect around the 1 molar equivalent which is supporting evidence for a 1:1 binding ratio. The m/s data in Appendix A shows that the most abundant species is the 1:1 host-guest complex for all compounds based on relative peak intensities and isotopic patterns.

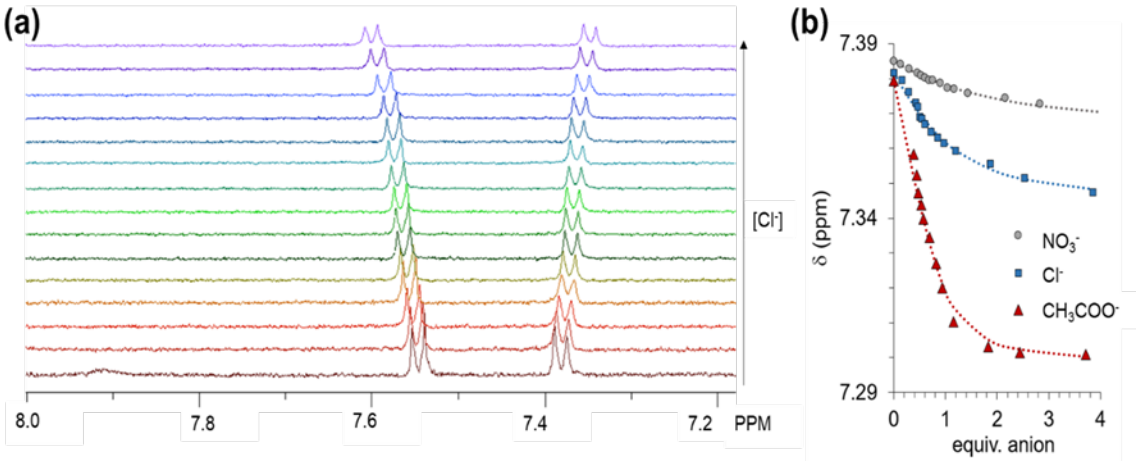

Figure 14 (a) Overlay of ^{1}H NMR spectra obtained during the titration of 1 (8.98 x 10^{-5} M in CD_3CN) with $[Bu_4N]Cl$. (b) Comparison of ^{1}H NMR chemical shifting observed during titration of 1 with nitrate, chloride, and acetate anions. The dotted lines represent the results of non-linear fitting to a 1:1 host–guest binding model

Unfortunately, the N-H signal experienced broadening because of the low concentration (≈ 1 x 10^{-4} M), and as a result the aromatic proton chemical shifts were used to probe binding behavior. The two unique aromatic proton chemical shifts observed for compounds 1-4, are a result of a protons nearest the urea moiety (H_α) and the protons nearest the NC functional group (H_β). The protons closer to the urea moiety (H_α) show up more down field than the protons closer to the NC moiety. The (H_α) signal also experienced broadening therefor, the (H_β) signal was used to determine K_a for all host–guest complexes. Figure 14a illustrates the effects of chloride titration on the aromatic ^{1}H NMR signals of 1a, while Figure 14b compares the magnitude of the ^{1}H NMR chemical shifts observed upon titration of 1a with the different anions nitrate, chloride, and acetate anions. Figure 15 details the magnitude of the ^{1}H NMR chemical shift for complexes 2a, 3a, and 4a. A similar trend is seen by all molecules and the corresponding anions. From Figure 14b and Figure 15 it is clear to see that the chemical shifts change as the anions change from NO_3^- < Cl^- < CH_3COO^-.

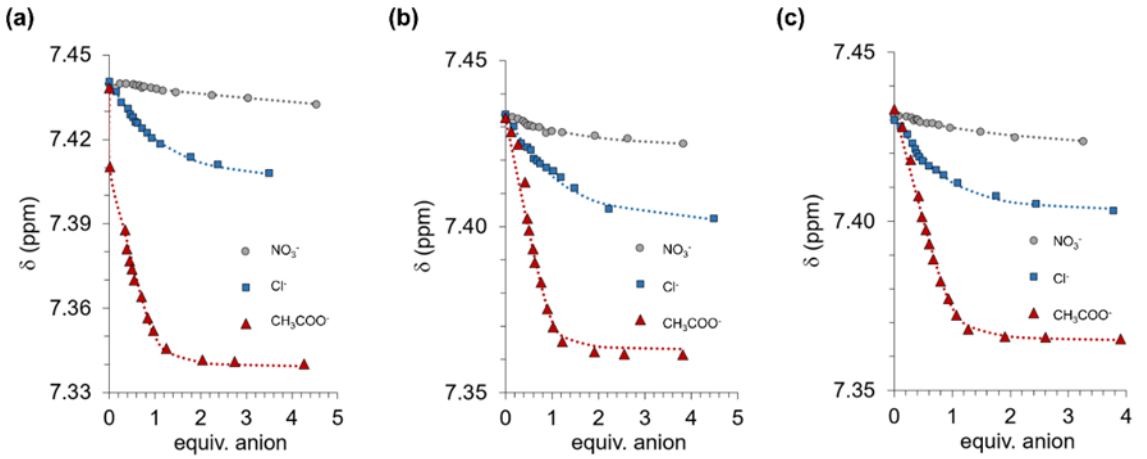

Figure 15 ^{1}H NMR chemical shifting observed during titration of (a) 2a, (b) 3a, and (c) 4a (~ 0.1 mM in CD_3CN) with nitrate, chloride, and acetate anions. The dotted lines represent the results of non-linear fitting to a 1:1 host–guest binding model

The titration study confirms that anion binding is a strong feature of the urea moiety even with the addition of multiple metal carbonyls attached to the molecule. The binding constants from compounds 1a, 2a, 3a, and 4a are in the magnitude of 10^3, 10^4, and 10^5 as tabulated in **Table 3** which is interestig because it provides enough support to potentially pursure anion binding as a method of templating. Anion binding could be used as a possible method of coordinating multiple units together if more than one urea moeity were present in the system which could potentially bring multiple metal carbonyls within close proximity to build non-traditional MCCs through secondary interactions.

Table 3 **Equilibrium constants (log K) for formation of host—guest complexes of 1-4 with selected anions.**

	log *K* [a]		
Urea Host	**NO_3^-**	**Cl^-**	**CH_3COO^-**
1a	3.62(5)	4.42(3)	5.30(8)
2a	3.52(3)	4.35(3)	5.41(7)
3a	3.60(3)	4.35(8)	5.50(3)
4a	3.70(3)	4.58(3)	5.66(4)

[a] In CD_3CN solution at 25 °C. Values in parentheses indicate uncertainty in the last figure

2.3 Conclusion

The characterization and synthesis of 1,3-bis(p-isocyanophenyl)urea and its group 6 metal containing derivatives provided sufficient data to lay a solid foundation for continuing research. The mostly planar conformation of the crystal structure is largely a result of the of the hydrogen bonding ability of the ortho proton closer to the oxygen molecule of the urea carbonyl. The urea pocket has a high affinity to bind anions at very low concentrations (10^{-3}, 10^{-4}, and 10^{-5} M). The crystal packing structure revealed the π-π interactions and urea-π interactions as the largest contributor to the molecular overlay. As a result of the crystal packing structure, it was observed that the appended group 6 metal centers are between 6.00 Å and 8.00 Å which is a distance that has the potential to allow for electrochemical communication.

CHAPTER THREE: FINAL STATEMENTS

3.1 Conclusion

Throughout the duration of this project, I have been able to develop a method that allows for organic molecules with the ability to self-assemble to be appended to low-valent metal carbonyls. A thorough study of the molecular organization revealed important foundational information about the role of π -stacking and urea- π stacking in the molecular crystal structure. The crystal structures allowed me to see the preferred method of organization as well as determine which features contribute the most to the organization patterns. The appended metal carbonyls are in close proximity in the solid state to suggestion potential for electronic communication. The titration studies revealed a strong affinity to bind anions at the urea hydrogens which opens the door to continuing research to unlock different binding ratios with the incorporation of multiple urea moieties or to pursue co-crystallization with an anion to alter the molecular crystal packing.

3.2 Future Works

The results of this project allow for the continuation of this research in several different directions: 1. Alteration of the substitution of the aromatic rings of the *N,N'*-diarylurea moiety can change the conformation from mostly planar to something different which may unlock new crystal packing organization patterns. 2. Appending larger premade MCCs to the organic linking molecule to increase the overall metal nuclearity. 3. Changing the urea group to another known self-assembling moiety. 4. Continuing with anion binding studies to explore different potential binding ratios or crystal packing organizations.

Regardless, additional research should be put into the field of understanding supramolecular interactions of metal carbonyl complexes and the facilitating role that self-assembling agents possess.

CHAPTER FOUR: EXPERIMENTAL

General Considerations. All synthetic operations were carried out under a nitrogen atmosphere using standard Schlenk techniques to exclude moisture and oxygen. Nitrogen was prepurified by passage through columns of activated copper catalyst (BASF PuriStar R3-11G) and molecular sieves (RCI-DRI 13X). Glassware was dried in an oven at 130 °C, assembled while hot, and allowed to cool under reduced pressure. All solvents were dried according to published procedures and degassed with nitrogen prior to use.[44] $Cr(CO)_6$ (Beantown Chemical, 99%), $Mo(CO)_6$ (Acros, 98%), $W(CO)_6$ (Beantown Chemical, 97%), PdO (Acros), trimethylamine N-oxide dihydrate (Beantown Chemical, 98%), and triphosgene (Chem Impex, 99%) were used as received without further purification. 4-isocyanophenylamine was prepared according to literature procedures and sublimed prior to use.[33]

Infrared spectra were obtained using a Thermo Scientific Nicolet iS5 FTIR spectrometer equipped with a 0.2 mm BaF_2 liquid cell. ^1H and ^{13}C NMR data were recorded on a 600 MHz Bruker AVANCE III spectrometer. Electrospray ionization mass spectrometry (ESIMS) was carried out using a Bruker HCTultra CTD II spectrometer in negative ion mode. Samples of **1-4** were dissolved in CH_3CN and treated with the tetrabutylammonium salts of chloride, nitrate, and acetate prior to injection into the mass spectrometer. Elemental analyses were performed by Atlantic Microlab, Inc in Norcross, GA, USA.

Synthesis of 1,3 bis(p isocyanophenyl)urea (1a). 4-isocyanophenylamine (3.00 g, 25.4 mmol) was dissolved in 80 mL of anhydrous dichloromethane, followed by addition of 7.8 mL of triethylamine. The solution was cooled to 0 °C and triphosgene (1.20 g, 4.04 mmol) was slowly introduced into the reaction vessel. (CAUTION: Triphosgene is toxic and its reaction with 4-isocyanophenylamine generates considerable heat and an abundance of hydrogen chloride. Triphosgene should be added very slowly and in several portions to allow for sufficient heat exchange with the cooling media.) The light yellow reaction mixture was magnetically stirred for 3 hours at 0 °C, then stirred for an additional 45 hours at 25 °C. Methanol (10 mL) was added to the reaction mixture and stirring was continued for an additional hour. Organic solvents were removed under reduced pressure, and the residues were dissolved in 60 mL of dimethyl formamide (DMF). Deionized water (60 mL) was slowly added, and the reaction vessel was gently heated to ensure that the solution remained clear. After addition of deionized water, the solution was allowed to cool slowly to room temperature, whereupon an off-white precipitate formed. The precipitate was filtered and washed with three 20 mL portions of water, followed by 20 mL of diethyl ether and 20 mL of hexanes, respectively. After drying under reduced pressure for one day, 1 was obtained with sufficient purity for further experimentation. Yield: 2.82 g (84.6%). IR (CH_2Cl_2, cm^{-1}): ν_{CN} 2027 (vs). ^1H NMR (CD_3CN, 20 °C): δ 7.38 (d, 4H, Ar–H, J = 8.86 Hz), 7.53 (d, 4H, Ar–H, J = 8.86 Hz), 7.60 (br s, 2H, N–H). ^{13}C NMR (CD_3CN, 20 °C): δ 119.3, 127.1, 140.3, 151.9, 163.5, ipso C not observed. MS(ESI): m/z 297 $[M + Cl^-]^-$, 324 $[M + NO_3^-]^-$, 321 $[M + CH_3COO^-]^-$. Anal. Calcd for $C_{15}H_{10}N_4O$: C, 68.69; H, 3.84; N, 21.36. Found: C, 68.47; H, 4.05; N, 21.17.

Synthesis of 1-(isocyanophenyl)urea (1b). 4-Isocyanophenylamine (2.67 mmol, 318 mg) and 4-isocyanophenylamine (2.54 mmol, 300 mg) were added to a standard Schlenk flask and dissolved in 20 mL of CH_3CN. The flask was refluxed for 3 h. After reflux, the flask was cooled to rt and the solvent was removed under reduced pressure. The product was extracted with toluene and filtered. The filtrate was washed with toluene followed by hexanes and dried under vacuum at 0 °C for several h. The pale yellow solid was transferred to a tared vial (433 mg, 72% yield). IR (CH_2Cl_2, cm^{-1}): $_{\nu CN}$ 2064 (w). ^1H NMR (600 MHz, CD_3CN, δ): 7.05 (t, *J* = 7.41 Hz, 1H, Ar H), 7.31 (t, *J* = 8.15 Hz, 2H, Ar H), 7.37 (m, 3H), 7.44 (d, *J* = 7.61 Hz, 2H, Ar H), 7.53 (d, *J* = 8.59 Hz, 2H Ar H), 7.55 (br s, 1H, NH). ^{13}C NMR (600 MHz, CD_3CN): δ 117.29, 119.01, 122.91, 127.06, 128.85, 139.07, 140.74, 152.29, 163.36, 206.47. MS(ESI): m/z 367.8 (M^+), 339.8 (M - CO), 311.8 (M - 2CO), 283.8 (M - 3CO), 255.8 (þ- 4CO), 227.8 (M- 5CO), 199.8 (M-6CO), 171.8 (M-7CO), 143.8 (M - 8CO).

Synthesis of Complex 2a. $Cr(CO)_6$ (317 mg, 1.44 mmol) and 1a (182 mg, 0.694 mmol) were combined with 25 mL of DMF and heated to 90 °C, whereupon PdO (14 mg, 0.12 mmol) was added to the reaction vessel. The reaction mixture was magnetically stirred at 90 °C for 15 minutes, then allowed to cool to room temperature. DMF was removed by vacuum distillation, leaving behind an oily residue. The oily residue was extracted with dichloromethane and filtered to remove insoluble impurities. Hexanes were added slowly to the dichloromethane filtrate until the solution became cloudy, then the solution was centrifuged at 5000 rpm for 2 minutes, after which the clear supernatant was decanted and dried under reduced pressure. The residual pale yellow solid was dissolved in warm acetonitrile, then cooled slowly to -20 °C to yield crystals of 2•CH_3CN. Yield: 242 mg

(50.7%). IR (CH_2Cl_2, cm^{-1}): νCN 2143 (m), νCO 2058 (s), 1955 (vs). ^1H NMR (CD_3CN, 20 °C): δ 7.43 (d, 4H, Ar–H, J = 8.75 Hz), 7.58 (d, 4H, Ar–H, J = 8.89 Hz), 7.71 (br s, 2H, N–H). ^{13}C NMR (CD_3CN, 20 °C): δ 120.2, 127.9, 141.1, 153.0, isocyanide and adjacent ipso carbons not observed. MS(ESI): m/z 681 $[M + Cl^-]^-$, 708 $[M + NO_3^-]^-$, 705 $[M + CH_3COO^-]^-$. Anal. Calcd for $C_{27}H_{13}Cr_2N_5O_{11}$: C, 47.18; H, 1.91; N, 10.19. Found: C, 47.23; H, 1.83; N, 10.16.

Synthesis of Complex 3a. $Mo(CO)_6$ (811 mg, 3.07 mmol) and 1a (403 mg, 1.54 mmol) were dissolved in 25 mL of tetrahydrofuran (THF). A dropping funnel charged with trimethylamine N-oxide dihydrate (342 mg, 3.07 mmol), THF (10 mL), and methanol (10 mL) was attached to the reaction flask, the contents of which were added dropwise to the reaction mixture over the course of 1 hour. The reaction mixture was magnetically stirred for 6 hours at room temperature, after which the solvents were removed under reduced pressure. The residues were extracted with dichloromethane and filtered to remove insoluble impurities. Hexanes were added slowly to the dichloromethane filtrate until the solution became cloudy, then the solution was centrifuged at 5000 rpm for 2 minutes, after which the clear supernatant was decanted and dried under reduced pressure. The residual off-white solid was dissolved in warm acetonitrile, then cooled slowly to -20 °C to yield crystals of 3a. Yield: 871 mg (77.0%). IR (CH_2Cl_2, cm^{-1}): νCN 2143 (m), νCO 2063 (s), 1956 (vs). ^1H NMR (CD_3CN, 20 °C): δ 7.38 (d, 4H, Ar–H, J = 8.88 Hz), 7.53 (d, 4H, Ar–H, J = 8.84 Hz), 7.60 (br s, 2H, N–H). ^{13}C NMR (CD_3CN, 20 °C): δ 119.3, 127.2, 140.4, 151.8, isocyanide and adjacent ipso carbons not observed. MS(ESI): m/z 769 $[M + Cl^-]^-$, 796 $[M + NO_3^-]^-$, 793 $[M + CH3COO^-]^-$. Anal. Calcd for $C_{25}H_{10}Mo_2N_4O_{11}$: C, 40.89; H, 1.37; N, 7.63. Found: C, 41.03; H, 1.38; N, 8.15.

Synthesis of Complex 3b. $Mo(CO)_6$ (556 mg, 2.10 mmol) and 1b (500 mg, 2.10 mmol) were dissolved in 25 mL of tetrahydrofuran (THF). A dropping funnel charged with trimethylamine N-oxide dihydrate (233 mg, 2.10 mmol), THF (10 mL), and methanol (10 mL) was attached to the reaction flask, the contents of which were added dropwise to the reaction mixture over the course of 1 hour. The reaction mixture was magnetically stirred for 6 hours at room temperature, after which the solvents were removed under reduced pressure. The residues were extracted with ethyl acetate and filtered to remove insoluble impurities. The filtrate was adsorbed onto silica then run through a column (50% CH_2Cl_2/ 40% hex/10% EtOAc), after which the solvents were removed under reduced pressure. The residues were resuspended with dimethylformamide (DMF) and then slowly titrated with water to produce crystalline needles of 3b. Yield: 606 mg (60.7%). IR (CH_2Cl_2, cm^{-1}): νCN 2143 (m), νCO 2063 (s), 1956 (vs). ^1H NMR (CD_3CN, 20 °C): δ 7.05 (t, 1H, Ar–H, J = 7.41 Hz), 7.31 (t, 2H, Ar–H, J = 8.15 Hz), 7.40 (m, 3H), 7.45 (d, *J* = 7.61 Hz, 2H, Ar H), 7.55 (d, *J* = 8.59 Hz, 2H Ar H), 7.61 (br s, 1H, N–H). ^{13}C NMR (CD_3CN, 20 °C): δ 119.3, 127.2, 140.4, 151.8, isocyanide and adjacent ipso carbons not observed. MS(ESI): m/z 474. Anal. Calcd for $C_{25}H_{10}Mo_2N_4O_{11}$: C, 40.89; H, 1.37; N, 7.63. Found: C, 41.03; H, 1.38; N, 8.15

Synthesis of Complex 4a. $W(CO)_6$ (369 mg, 1.05 mmol) and 1a (132 mg, 0.503 mmol) were combined with 25 mL of DMF and heated to 90 °C, whereupon PdO (10 mg, 0.082 mmol) was added to the reaction vessel. The reaction mixture was magnetically stirred at 90 °C for 5 minutes, then cooled to room temperature. DMF was removed by vacuum distillation, leaving behind an oily residue. The oily residue was extracted with dichloromethane and filtered to remove insoluble impurities. Hexanes were added slowly

to the dichloromethane filtrate until the solution became cloudy, then the solution was centrifuged at 5000 rpm for 2 minutes, after which the clear supernatant was decanted and dried under reduced pressure. The residual yellow solid was dissolved in warm acetonitrile, then cooled slowly to -20 °C to yield crystals of 4a. Yield: 211 mg (44.1%). IR (CH_2Cl_2, cm^{-1}): ν_{CN} 2144 (m), ν_{CO} 2059 (s), 1950 (vs). ^1H NMR (CD_3CN, 20 °C): δ 7.43 (d, 4H, Ar–H, J = 8.93 Hz), 7.57 (d, 4H, Ar–H, J = 9.00 Hz), 7.69 (br s, 2H, N–H). ^{13}C NMR (CD_3CN, 20 °C): δ 119.3, 127.3, 140.4, 151.8, isocyanide and adjacent ipso carbons not observed. MS(ESI): m/z 945 $[M + Cl^-]^-$, 972 $[M + NO_3^-]^-$, 969 $[M + CH3COO^-]^-$. Anal. Calcd for $C_{27}H_{13}N_5O_{11}W_2$: C, 34.10; H, 1.38; N, 7.36. Found: C, 34.29; H, 1.31; N, 7.41.

Determination of Equilibrium Formation Constants (K) by ^1H NMR. In typical titration experiments, CD_3CN solutions of urea hosts 1-4 (0.75 mL, 0.10 mM) were loaded into standard NMR tubes and initial ^1H NMR spectra were collected. Fourteen aliquots of an anion-containing solution were then delivered to the NMR tubes using a microsyringe, the mass of each aliquot being recorded on a microbalance. The first ten aliquots of titrant were taken from a stock solution of the anion guest (2.0 mM) prepared by dissolving a known quantity of the appropriate tetrabutylammonium salt in a 0.10 mM solution of the urea host, thereby minimizing host dilution effects. The final four aliquots were taken from a stock solution of anion guest (4.0 mM) prepared in the same manner. Sufficient anion was delivered during each titration step to enable collection of ^1H NMR spectra at the following approximate [anion]/[urea] ratios: 0.1, 0.2, 0.3, 0.4, 0.5, 0.6, 0.7, 0.8, 0.9, 1.0, 1.2, 2.0, 3.0, and 4.0. The upfield shifting of the aromatic proton signals centered between 7.38–7.43 ppm was recorded and values of K were calculated by non-linear fitting to a 1:1 binding model using the WinEQNMR2 software package.[45]

Crystal Structure Determination of Complexes 2-4. X-ray diffraction data were collected at 100 K on a Bruker D8 Venture using MoKα-radiation (λ = 0.71073 Å). Data were corrected for absorption effects using the SADABS area detector absorption correction program.[46] The structures were solved by direct methods using Olex2 with the SHELXT structure solution program and refined with the SHELXL refinement package using least squares minimization.[47–49] All non-hydrogen atoms were refined with anisotropic thermal parameters. Hydrogen atoms attached to heteroatoms were identified from the residual density maps and refined with isotropic thermal parameters. All other hydrogen atoms in the investigated structure were located from difference Fourier maps, but their positions were ultimately placed in geometrically calculated positions and refined using a riding model. Additional calculations and refinement of structures were carried out using APEX3 and SHELXTL software.[50] Graphical representations of crystallographic data were generated using the Mercury software package.[51] X-ray data collection and refinement parameters are tabulated in Table 4.

Electrochemical Measurements. Cyclic voltammograms were recorded in 0.1 M $[Bu_4N][PF_6]$ DMF solutions at v = 100 mV/sec with a Princeton Applied Research VersaSTAT 3 potentiostat. All experiments were performed using a standard three-electrode configuration under an atmosphere of pure nitrogen. Glassy carbon working electrodes (3 mm, CH Instruments) were used for all measurements and were polished with aqueous slurries of 0.3 μm and 0.05 μm alumina powder, sequentially. After polishing, the electrodes were rinsed with Milli-Q water, methanol, and dichloromethane and dried in a stream of air. Working electrodes were preconditioned by performing three cyclical scans from 2.0 to -2.5 V at 250 mV/sec in a DMF solution of $[Bu_4N][PF_6]$ (0.1

M). A graphite rod served as the counter electrode and a silver wire immersed in a 0.1 M DMF solution of $[Bu_4N][PF_6]$ and separated from the cell compartment by a porous glass frit (CoralPor 1000) was employed as a Ag^+/Ag pseudoreference electrode. Measured potentials are reported relative to the ferrocenium(1+)/ferrocene(0) redox couple, which was achieved by addition of ferrocene at the end of each set of scans.

Table 4 **X-ray data collection and refinement parameters for complexes 2a, 3a, and 4a.**

Compound	**2a**	**3a**	**4a**	
Formula	$C_{27}H_{13}Cr_2N_5O_{11}$	$C_{27}H_{13}Mo_2N_5O_{11}$	$C_{27}H_{13}N_5O_{11}W_2$	Monosubsssss species
Formula weight	687.42	775.30	951.12	
Temperature (K)	100	100	100	
Crystal system	monoclinic	monoclinic	monoclinic	
Space group	$P2_1/c$	$P2_1/c$	$P2_1/c$	
***a* (Å)**	6.8126(2)	6.8694(5)	6.8575(4)	
***b* (Å)**	13.8536(5)	14.0047(10)	13.9691(9)	
***c* (Å)**	32.1439(11)	32.536(2)	32.525(2)	
***α* (deg)**	90	90	90	
***β* (deg)**	93.8630(10)	93.115(2)	93.145(2)	
***γ* (deg)**	90	90	90	
Volume ($Å^3$)	3026.82(17)	3125.5(4)	3110.9(3)	
Z	4	4	4	
density ($g/cm^{3)}$	1.509	1.648	2.031	
abs coeff (mm^{-1})	0.784	0.867	7.454	
F(000)	1384	1528	1784	
Crystal size (mm)	0.42 × 0.18 × 0.12	0.4 × 0.05 × 0.05	0.17 × 0.14 × 0.05	
λ (MoKα) (Å)	0.71073	0.71073	0.71073	
2θ range (deg)	5.87 to 55.068	5.818 to 61.12	5.804 to 54.968	
reflns (coll)	40623	120953	50308	
reflns (unique)	6937	9565	7120	
Data/restraints/parameters	6937/0/415	9565/0/415	7120/0/415	
GOF (on F^2)	1.131	1.072	1.206	
Final R indexes [I ≥ 2σ (I)]	R_1 = 0.0356, wR_2 = 0.0848	R_1 = 0.0327, wR_2 = 0.0578	R_1 = 0.0242, wR_2 = 0.0463	
Final R indexes [all data]	R_1 = 0.0433, wR_2 = 0.0877	R_1 = 0.0555, wR_2 = 0.0623	R_1 = 0.0312, wR_2 = 0.0477	
Largest diff. peak/hole (e $Å^{-3}$)	0.45/-0.23	0.58/-0.47	0.88/-0.43	

REFERENCES

1. Shriver, D. F., Kaesz, H. D., Adams, R. D. *The Chemistry of Metal Cluster Complexes*. (1990).

2. Cotton, F. A., Zingales, F. The Donor–Acceptor Properties of Isonitriles as Estimated by Infrared Study. *J. Am. Chem. Soc.* **1961**, 83, 351–355.

3. Thimmappa, B. H. S., Low valent metal clusters — an overview., *Coor Chem. Rev*, **1995**, 143, 1-34.

4. Hogarth, G., Kabir, S. E. & Nordlander, E. Cluster chemistry in the Noughties: New developments and their relationship to nanoparticles. *Dalt. Trans.* **2010**, 39, 6153–6174.

5. Zacchini, S. Using metal carbonyl clusters to develop a molecular approach towards metal nanoparticles. *Eur. J. Inorg. Chem.*, **2011**, 4125–4145.

6. Eady, C. R., Johnson, B. F. G., Lewis, J. The chemistry of polynuclear compounds. Part XXVI. Products of the pyrolysis of dodecacarbonyl-triangulo-triruthenium and -triosmium. *J. Chem. Soc. Dalt. Trans.* **1975**, 2606-2611.

7. Volz, N., Clayden, J. The urea renaissance. *Angew. Chemie - Int. Ed.*, **2011**, 50, 12148–12155.

8. Isare, B., Pensec, S., Raynal, M., Bouteiller, L. Bisurea-based supramolecular polymers: From structure to properties, *Comptes Rendus Chim.* **2016**, 19, 148–156.

9. Boiocchi, M. *et al.* Nature of urea-fluoride interaction: Incipient and definitive proton transfer. *J. Am. Chem. Soc.*, **2004,** 126, 16507–16514.

10. Custelcean, R., Moyer, B. A., Bryantsev, V. S., Hay, B. P. Anion coordination in metal-organic frameworks functionalized with urea hydrogen-bonding groups. *Cryst. Growth Des.* **2006**, 6, 555–563.

11. Custelcean, R. Crystal engineering with urea and thiourea hydrogen-bonding groups. *Chem. Commun.* **2008**, 295–307.

12. S̄wiergiel, J., Bouteiller, L., Jadzyn, J. Hierarchical Structure of Supramolecular Polymers Formed by N,N′-Di(2-ethylhexyl)urea in Solutions. *J. Phys. Chem. B* **2015**, 119, 12947–12953.

13. Hussain, S., Brotherhood, P. R., Judd, L. W., Davis, A. P. Diaxial Diureido Decalins as Compact, Efficient, and Tunable Anion Transporters. *J. Am. Chem. Soc* **2011**, 133, 1614–1617.

14. Gale, P., Gunnlaugsson, T., Amendola, V., Fabbrizzi, L., Mosca, L. Supramolecular chemistry of anionic species themed issue Anion recognition by hydrogen bonding: urea-based receptorsw. *Chem. Soc. Rev* **2010**, 39, 3889.

15. Solomos, M. A., Watts, T. A., Swift, J. A. Predicting Cocrystallization Based on Heterodimer Energies: Part II., **2017**.

16. Etter, M. C., Reutzel, S. M. Hydrogen Bond Directed Cocrystallization and Molecular Recognition Properties of Acyclic Amides. *J. Am. Chem. Soc.* **1991**, 113, 2586–2589.

17. Janiak, C. A critical account on π–π stacking in metal complexes with aromatic nitrogen-containing ligands. *J. Chem. Soc. Dalt. Trans.* **2000**, 3885–3896.

18. Clayden, J., Hennecke, U., Vincent, M. A., Hillier, I. H., Helliwell, M. The origin of the conformational preference of N,N′-diaryl-N,N′-dimethyl ureas. *Phys. Chem. Chem. Phys.* **2010**, 12, 15056.

19. Ricks, H. L., Shimizu, L. S., Smith, M. D., Bunz, U. H. F., Shimizu, K. D. An N,N' -diaryl urea based conjugated polymer model system, *Tetrahedron Letters*.

20. Leach, P. A., Geib, S. J., Ii, J. A. C., Warnock, G. F., Cooper, N. J. Synthesis and Structural Characterization of [Co{CN(2,6-C6H3Me2)}4], the First Transition Metal Isonitrilate. *J. Am. Chem. Soc*, **1994**, 116.

21. Figgis, B. N. *et al.* Contribution from the The Transition Metal-Isocyanide Bond. An Approximate Molecular Orbital Study. *Trans. Faraday Soc* **1975**, 14.

22. Sarapu, A. C., Fenske, R. F. Bromotricarbonylbis(methyl isocyanide)manganese Contribution from the Bonding Properties of the Methyl Isocyanide Ligand. A Single-Crystal X-Ray Diffraction and Molecular Orbital Study of Bromotricarbonylbis(methyl isocyanide)manganese, $Mn(CO)_3(CNCH_3)_2Br$. *Inorganic Chemistry*, **1972**, 11.

23. King, R. B., Singh Saran, M. Isocyanide-Metal Complexes. II. CO and CN Stretching Modes in tert-Butyl Isocyanide Derivatives of the Octahedral Metal Carbonyls. *Inorganic Chemistry* **1974**, 13.

24. Carpenter, A. E., Rheingold, A. L., Figueroa, J. S. A Well-Defined Isocyano Analogue of HCo(CO) 4. 1: Synthesis, Decomposition, and Catalytic 1,1-Hydrogenation of Isocyanides. *Organometallics* **2016**, 35.

25. Angelici, R. J., Lazar, M. Isocyanide Ligands Adsorbed on Metal Surfaces: Applications in Catalysis, Nanochemistry, and Molecular Electronics, *Inorg. Chem*, **2008**, 47, 20, 9155-9165.

26. Spessard, G. O., Miessler, G. L. *Organometallic Chemistry*. New York, 2010; pp 75-92.

27. Femoni, C., Iapalucci, M. C., Kaswalder, F., Longoni, G., Zacchini, S. The possible role of metal carbonyl clusters in nanoscience and nanotechnologies. *Coord. Chem. Rev.* **2006**, 250, 1580–1604.

28. Varshey, D. B., Sander, J. R. G., Friscic, T., MacGillivray, L. R. Suprmolecular Interactions. in Supramolecular Chemistry: From Moleculaes to Nanomaterials **2012**.

29. Schneider, H. J. Binding mechanisms in supramolecular complexes. *Angew. Chemie - Int. Ed.* **2009**, 48, 3924–3977.

30. Gale, P. A., Steed, J. W. Supramolecular Chemistry: From Moleculaes to Nanomaterials. New York, **2012**.

31. Isare, B., Pembouong, G., Boué, F., Bouteiller, L. Conformational control of hydrogen-bonded aromatic bis-ureas. *Langmuir* **2012**, 28, 7535–7541.

32. Shikata, T. *et al.* Structure and dynamics of a bisurea-based supramolecular polymer in n-dodecane. *J. Phys. Chem. B* **2008**, 112, 8459–8465.

33. Heinze, K., Jacob, V. Stepwise Assembly of Mixed Metal Dinuclear Carbonyl Complexes. *Eur. J. Inorg. Chem.* **2003**, 3918–3923.

34. Hiscock, J. R., Gale, P. A., Hursthouse, M. B., Light, M. E., Jie, C. Z. Acyclic indole and carbazole-based sulfate receptors. *Chem. Sci.* **2010**, 1, 215.

35. Reddy, L. S., Chandran, S. K., George, S., Babu, N. J., Nangia, A. Crystal structures of N-aryl-N'-4-nitrophenyl ureas: Molecular conformation and weak interactions direct the strong hydrogen bond synthon. *Cryst. Growth Des.* **2007**, 7, 2675–2690.

36. Bryantsev, V. S., Firman, T. K., Hay, B. P. Conformational Analysis and Rotational Barriers of Alkyl-and Phenyl-Substituted Urea Derivatives. **2005**.

37. Etter, M. C., Urbañczyk-Lipkowska, Z., Zia-Ebrahimi, M., Panunto, T. W. Hydrogen Bond Directed Cocrystallization and Molecular Recognition Properties of Diarylureas. *J. Am. Chem. Soc* **1990**, 112.

38. Page, C. C., Moser, C. C., Chen, X., Dutton, P. L. Natural engineering principles of electron tunnelling in biological oxidation–reduction. *Nature,* **1999**. 402, 47–52.

39. Moser, C. C., Page, C. C.. Dutton, P. L. Darwin at the molecular scale: selection and variance in electron tunnelling proteins including cytochrome *c* oxidase. *Philos. Trans. R. Soc. B Biol. Sci.* **2006**, 361, 1295–1305.

40. Blažek Bregović, V., Basarić, N., Mlinarić-Majerski, K. Anion binding with urea and thiourea derivatives. *Coord. Chem. Rev.* **2015**, 295, 80–124.

41. Fischer, L., Guichard, G. Folding and self-assembly of aromatic and aliphatic urea oligomers: Towards connecting structure and function. *Org. Biomol. Chem.* **2010**, 8, 3102–3117.

42. Thordarson, P. Determining association constants from titration experiments in supramolecular chemistry. *Chem. Soc. Rev.* **2011**, 40, 1305–1323.

43. Brynn Hibbert, D. Thordarson, P. The death of the Job plot, transparency, open science and online tools, uncertainty estimation methods and other developments in supramolecular chemistry data analysis. *Chem. Commun.* **2016**, 52, 12792–12805.

44. Bradley, D., Williams, G., Lawton, M. Drying of Organic Solvents: Quantitative Evaluation of the Efficiency of Several Desiccants. *J. Org. Chem,* **2010**, 75, 8351.

45. Hynes, M. J. EQNMR: a computer program for the calculation of stability constants from nuclear magnetic resonance chemical shift data. *J. Chem. Soc. Dalt. Trans.* **1993**, 311.

46. SHELDRICK M., G. Program for Empirical Absorption Correction of Area Detector Data. *SADABS,* **1996**.

47. Dolomanov, O. V. *et al. OLEX2* : a complete structure solution, refinement and analysis program. *J. Appl. Crystallogr.* **2009**, 42, 339–341.

48. Sheldrick, G. M., IUCr. *SHELXT* – Integrated space-group and crystal-structure determination. *Acta Crystallogr. Sect. A Found. Adv.* **2015**, 71, 3–8.

49. Sheldrick, G. M. Crystal structure refinement with SHELXL. *Acta Crystallogr. Sect. C, Struct. Chem.* **2015**, 71, 3–8.

50. Sheldrick, G. M., IUCr. A short history of *SHELX*. *Acta Crystallogr. Sect. A Found. Crystallogr.* **2008**, 64, 112–122.

51. Macrae, C. F. *et al. Mercury CSD 2.0* – new features for the visualization and investigation of crystal structures. *J. Appl. Crystallogr.* **2008**, 41, 466–470.

APPENDIX A

Supporting Information

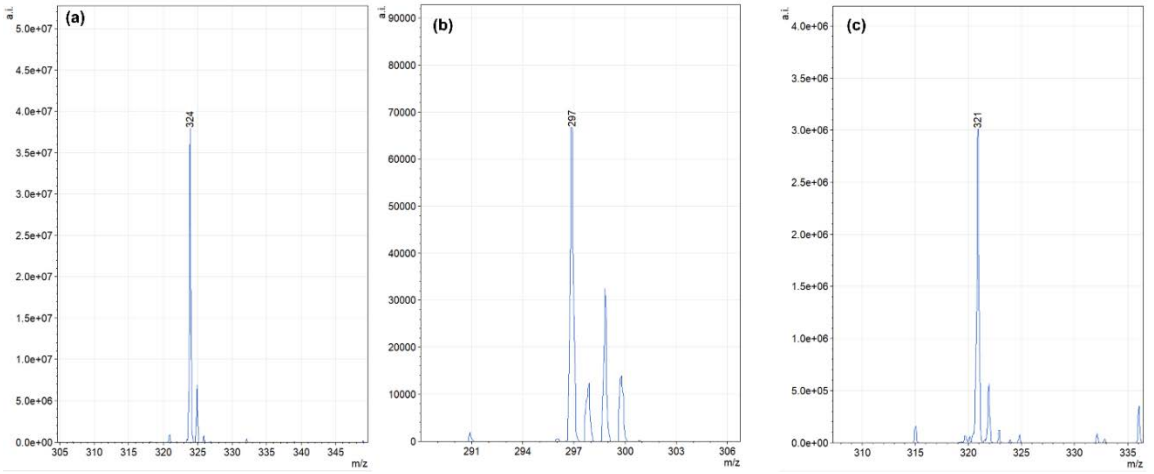

Figure S1. ESI-MS data for 1:1 host–guest complexes of 1a with (a) NO_3^- , (b) Cl^- , and (c) CH_3COO^-Figure S2. ESI-MS data for 1:1 host–guest complexes of 2a with (a) NO_3^- , (b) Cl^- , and (c) CH_3COO^-

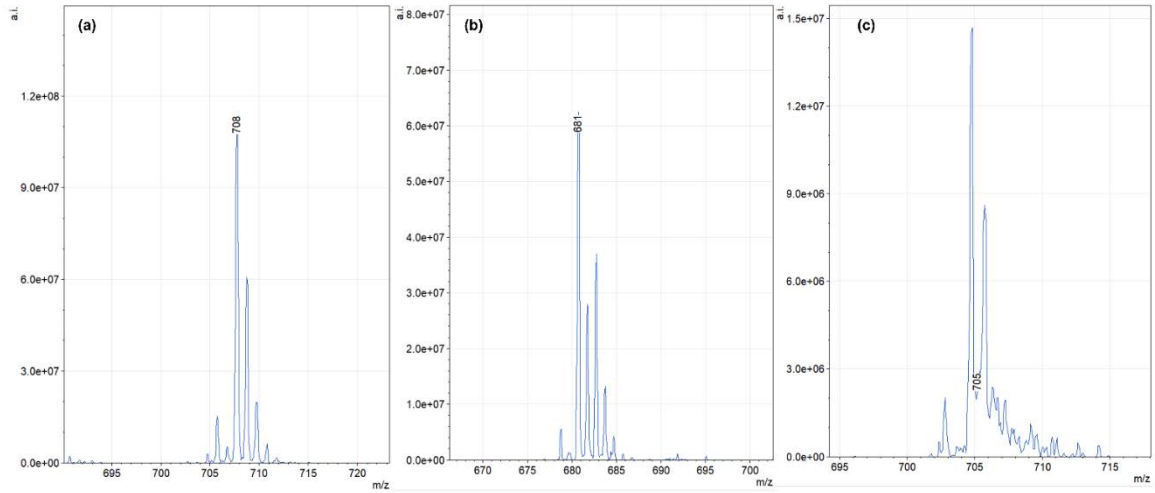

Figure S2. ESI-MS data for 1:1 host–guest complexes of 2a with (a) NO_3^- , (b) Cl^- , and (c) CH_3COO^-

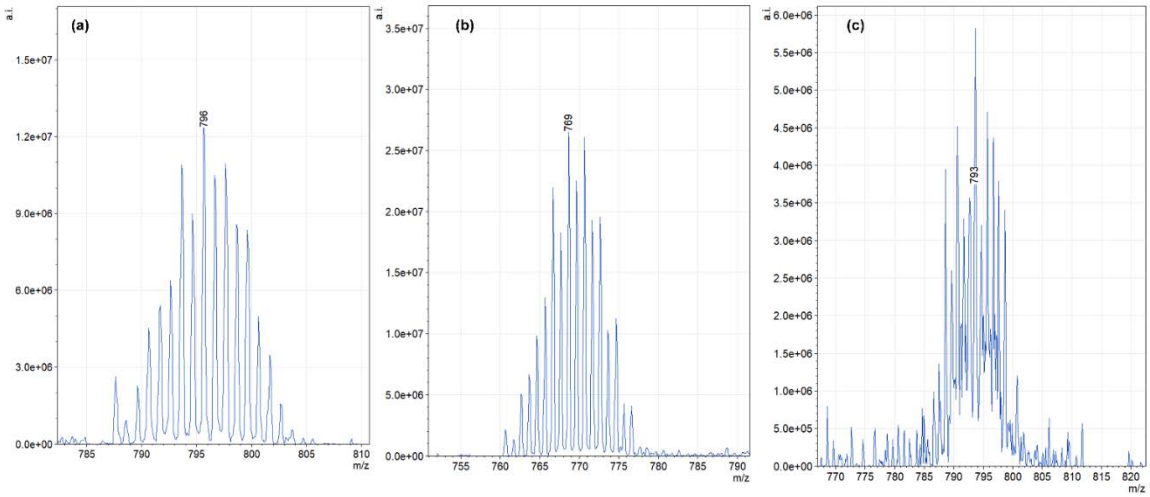

Figure S3. ESI-MS data for 1:1 host–guest complexes of 3a with (a) NO_3^- , (b) Cl^- , and (c) CH_3COO^-

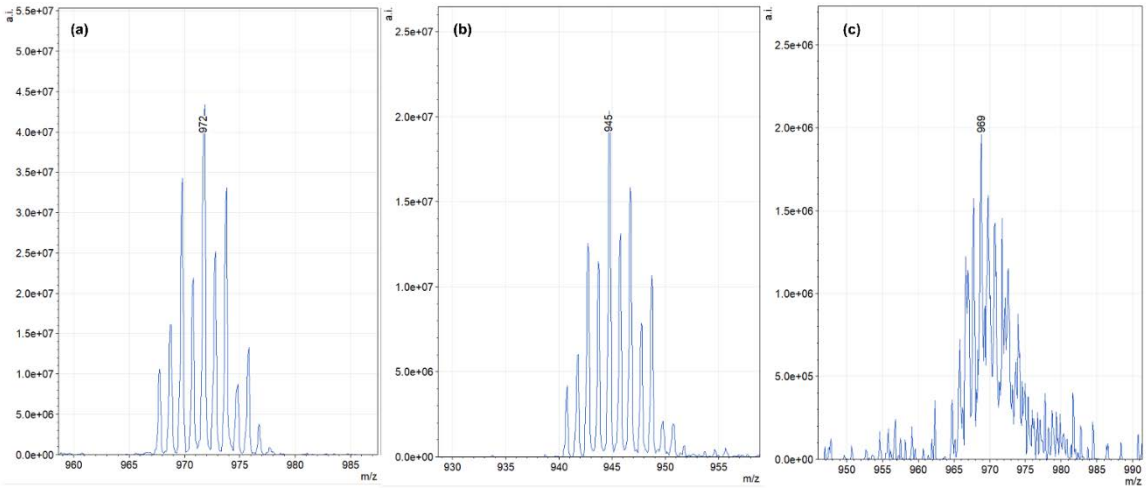

Figure S4. ESI-MS data for 1:1 host–guest complexes of 4 awith (a) NO_3^- , (b) Cl^- , and (c) CH_3COO^-

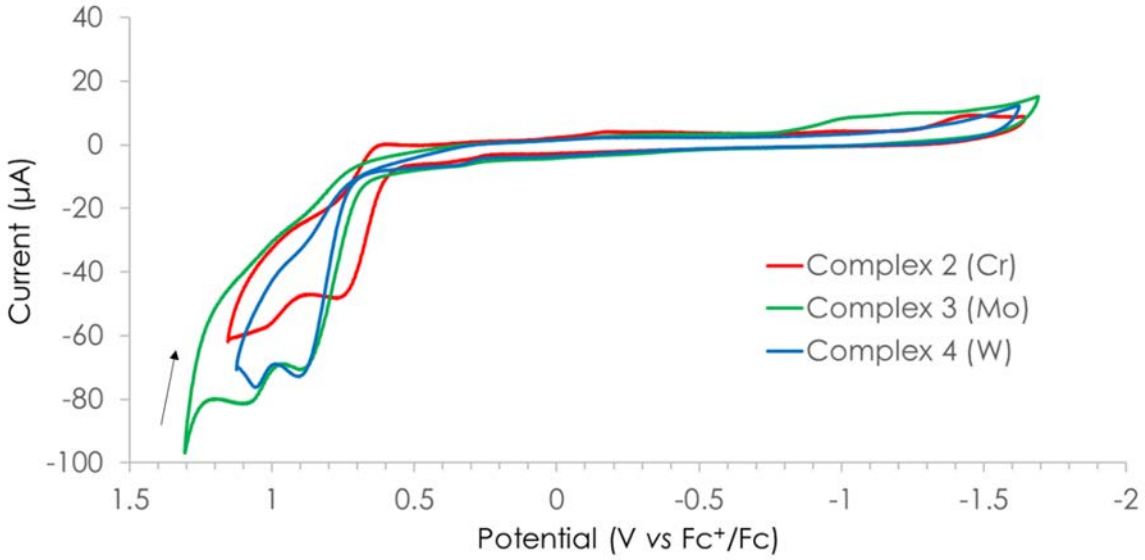

Figure S5. Cyclic voltammograms of complexes 2a, 3a, and 4a (≈ 1 mM) recorded in 0.1 M $[Bu_4N][PF_6]$ DMF solution at ν = 100 mV/sec with a glassy carbon working electrode, graphite rod counter electrode, and a silver wire pseudoreference electrode

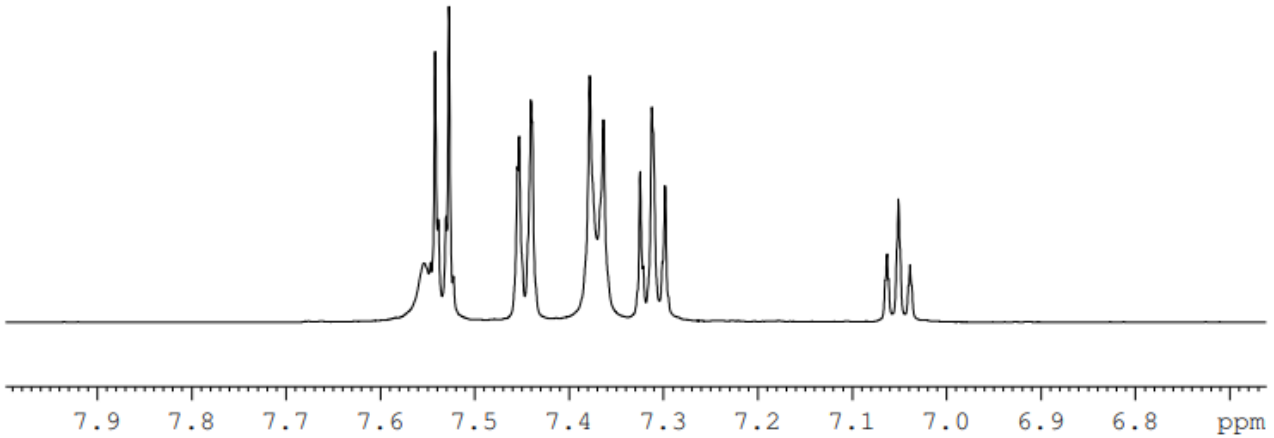

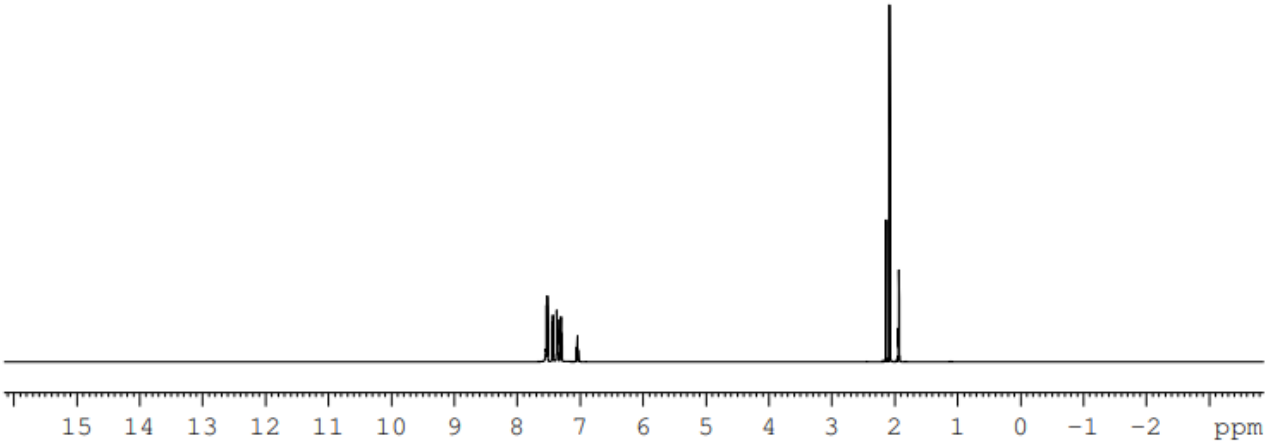

BRUKER

```
Current Data Parameters
NAME      Monosub Ligand Final
EXPNO                    1
PROCNO                   1

F2 - Acquisition Parameters
Date_           20190119
Time              16.07
INSTRUM           spect
PROBHD   5 mm PATXI 1H/
PULPROG            zg30
TD                65536
SOLVENT           CD3CN
NS                   16
DS                    2
SWH           12019.230 Hz
FIDRES         0.183399 Hz
AQ            2.7262976 sec
RG                  181
DW               41.600 usec
DE                6.50 usec
TE                298.1 K
D1           1.00000000 sec
TD0                  1

======== CHANNEL f1 ========
SFO1         600.1337060 MHz
NUC1                1H
P1                10.04 usec
PLW1         11.74899960 W

F2 - Processing parameters
SI                65536
SF           600.1300167 MHz
WDW                 EM
SSB       0
LB                0.30 Hz
GB        0
PC                1.00
```

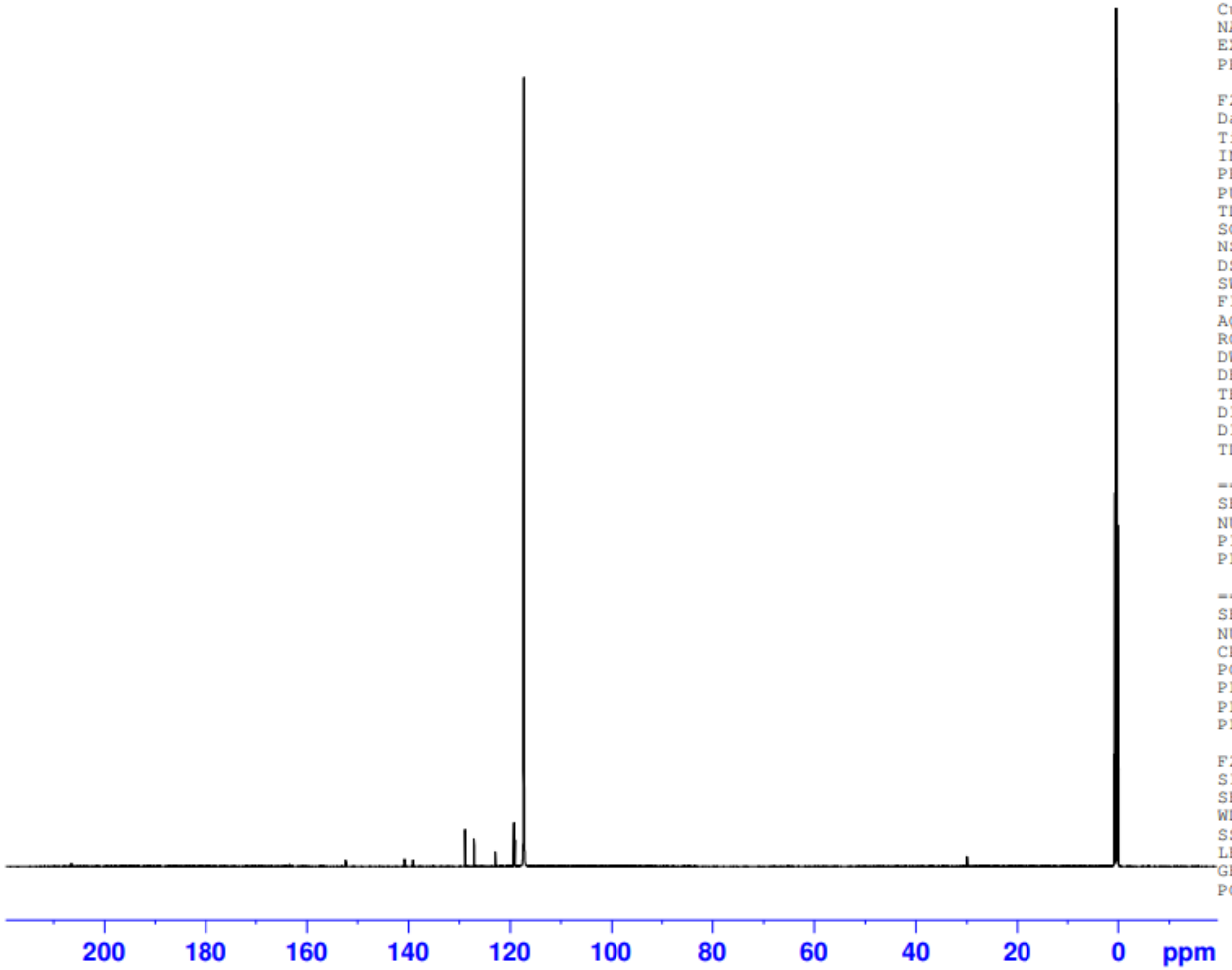


```
Current Data Parameters
NAME      Monosub Ligand Final
EXPNO                    2
PROCNO                   1

F2 - Acquisition Parameters
Date_           20190120
Time                9.04
INSTRUM            spect
PROBHD   5 mm PATXI 1H/
PULPROG          zgpg30
TD                65536
SOLVENT            CD3CN
NS                 20480
DS                     4
SWH            36057.691 Hz
FIDRES          0.550197 Hz
AQ             0.9087659 sec
RG                  2050
DW                13.867 usec
DE                  6.50 usec
TE                 298.1 K
D1            2.00000000 sec
D11           0.03000000 sec
TD0                    1

======== CHANNEL f1 ========
SFO1         150.9178981 MHz
NUC1                13C
P1                12.00 usec
PLW1        190.36999512 W

======== CHANNEL f2 ========
SFO2         600.1324005 MHz
NUC2                1H
CPDPRG[2         waltz16
PCPD2              70.00 usec
PLW2         11.74899960 W
PLW12         0.24169999 W
PLW13         0.12157000 W

F2 - Processing parameters
SI                 32768
SF           150.9028090 MHz
WDW                   EM
SSB       0
LB                 1.00 Hz
GB        0
PC                 1.40
```

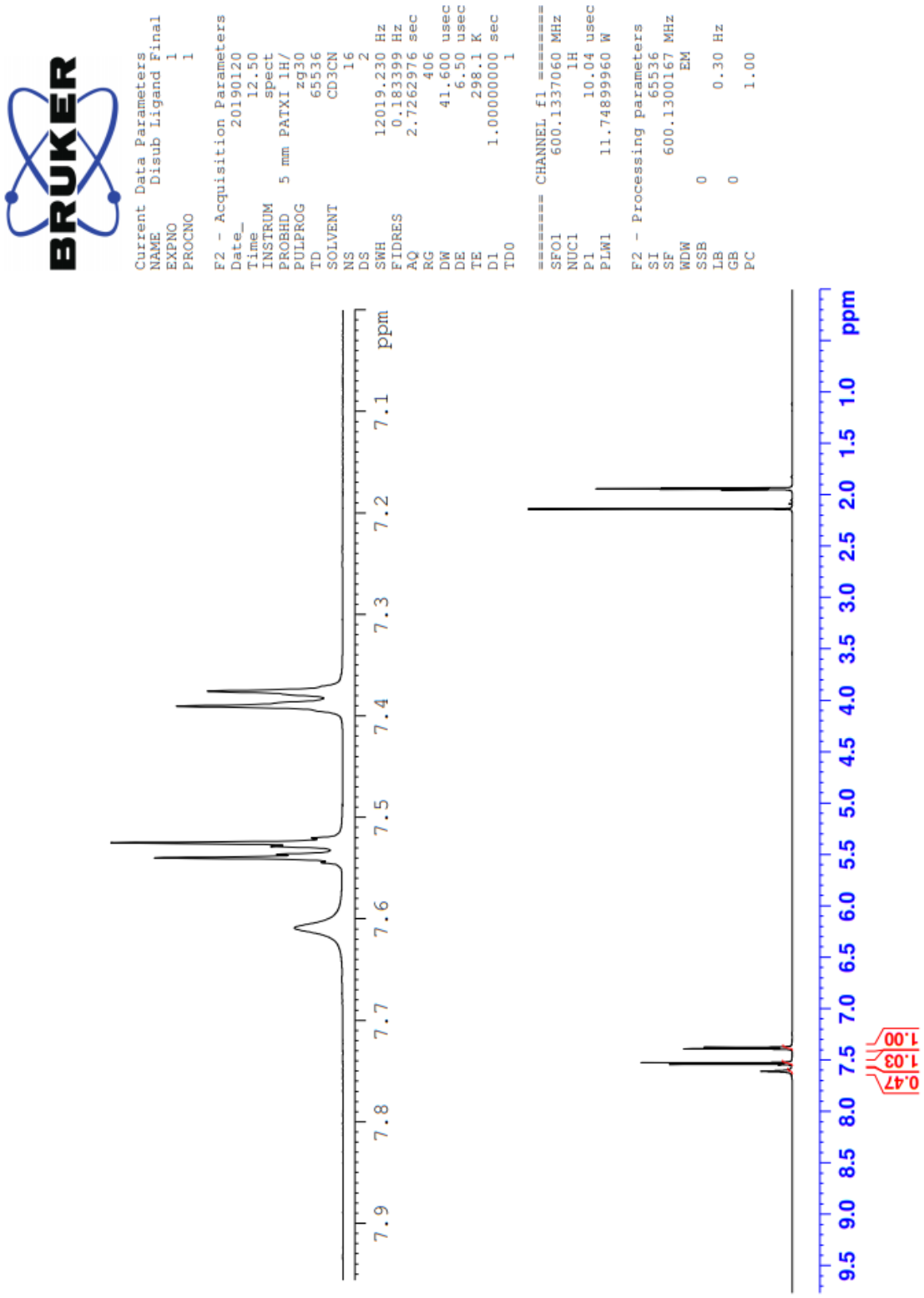
Current Data Parameters
NAME Disub Ligand Final
EXPNO 1
PROCNO 1
F2 - Acquisition Parameters
Date_ 20190120
Time 12.50
INSTRUM spect
PROBHD 5 mm PATXI 1H/
PULPROG zg30
TD 65536
SOLVENT CD3CN
NS 16
DS 2
SWH 12019.230 Hz
FIDRES 0.1833399 Hz
AQ 2.7262976 sec
RG 406
DW 41.600 usec
DE 6.50 usec
TE 298.1 K
D1 1.00000000 sec
TD0 1
======== CHANNEL f1 ========
SFO1 600.1337060 MHz
NUC1 1H
P1 10.04 usec
PLW1 11.74899960 W
F2 - Processing parameters
SI 65536
SF 600.1300167 MHz
WDW EM
SSB 0
LB 0.30 Hz
GB 0
PC 1.00
ppm
0.47
1.03
1.00

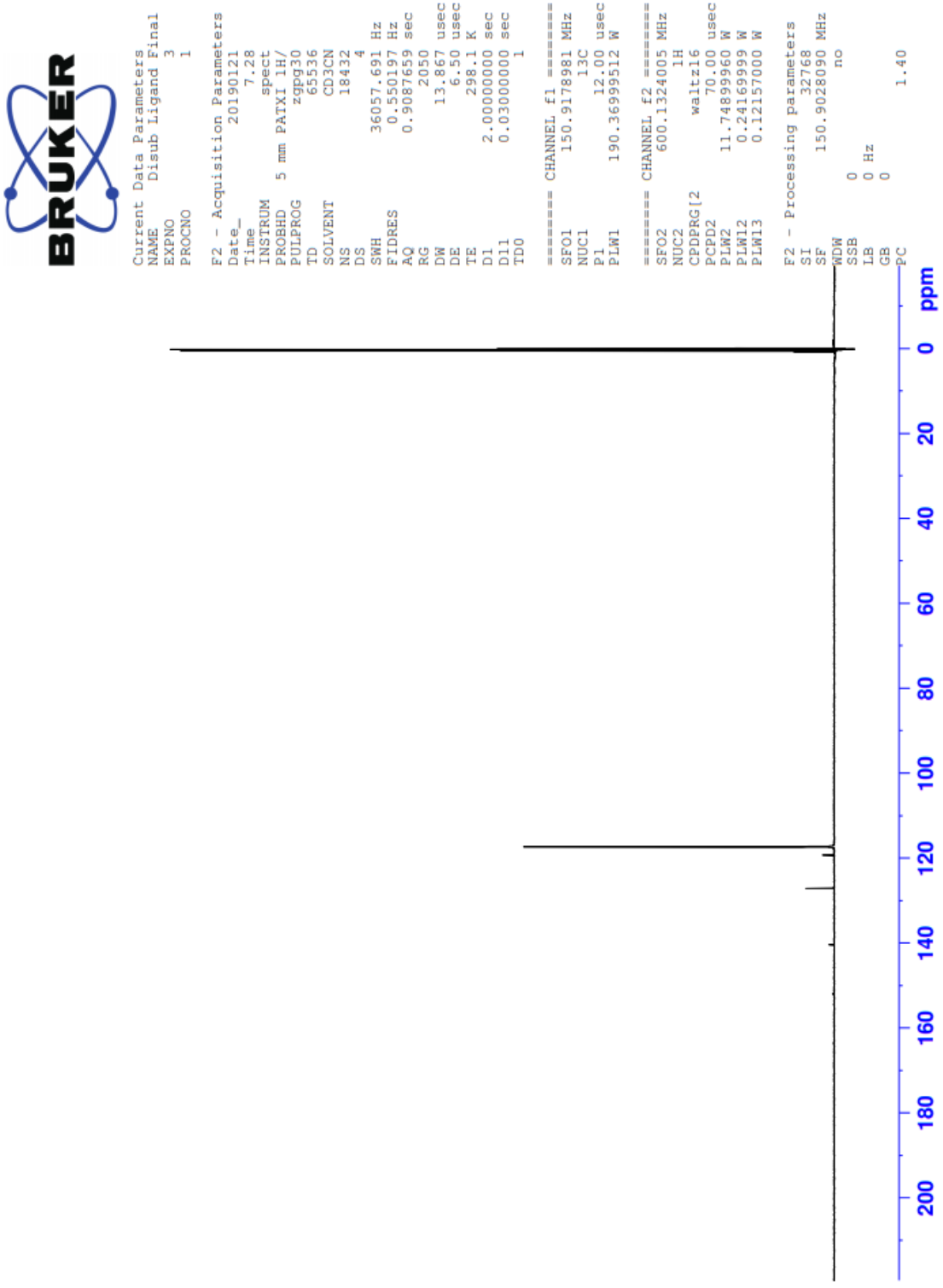
Current Data Parameters
NAME Disub Ligand Final
EXPNO 3
PROCNO 1
F2 - Acquisition Parameters
Date_ 20190121
Time 7.28
INSTRUM spect
PROBHD 5 mm PATXI 1H/
PULPROG zgpg30
TD 65536
SOLVENT CD3CN
NS 18432
DS 4
SWH 36057.691 Hz
FIDRES 0.550197 Hz
AQ 0.9087659 sec
RG 2050
DW 13.867 usec
DE 6.50 usec
TE 298.1 K
D1 2.00000000 sec
D11 0.03000000 sec
TD0 1
======== CHANNEL f1 ========
SFO1 150.9178981 MHz
NUC1 13C
P1 12.00 usec
PLW1 190.36999512 W
======== CHANNEL f2 ========
SFO2 600.1324005 MHz
NUC2 1H
CPDPRG[2 waltz16
PCPD2 70.00 usec
PLW2 11.74899960 W
PLW12 0.24169999 W
PLW13 0.12157000 W
F2 - Processing parameters
SI 32768
SF 150.9028090 MHz
WDW no
SSB 0
LB 0 Hz
GB 0
PC 1.40
200
180
160
140
120
100
80
60
40
20
0
ppm

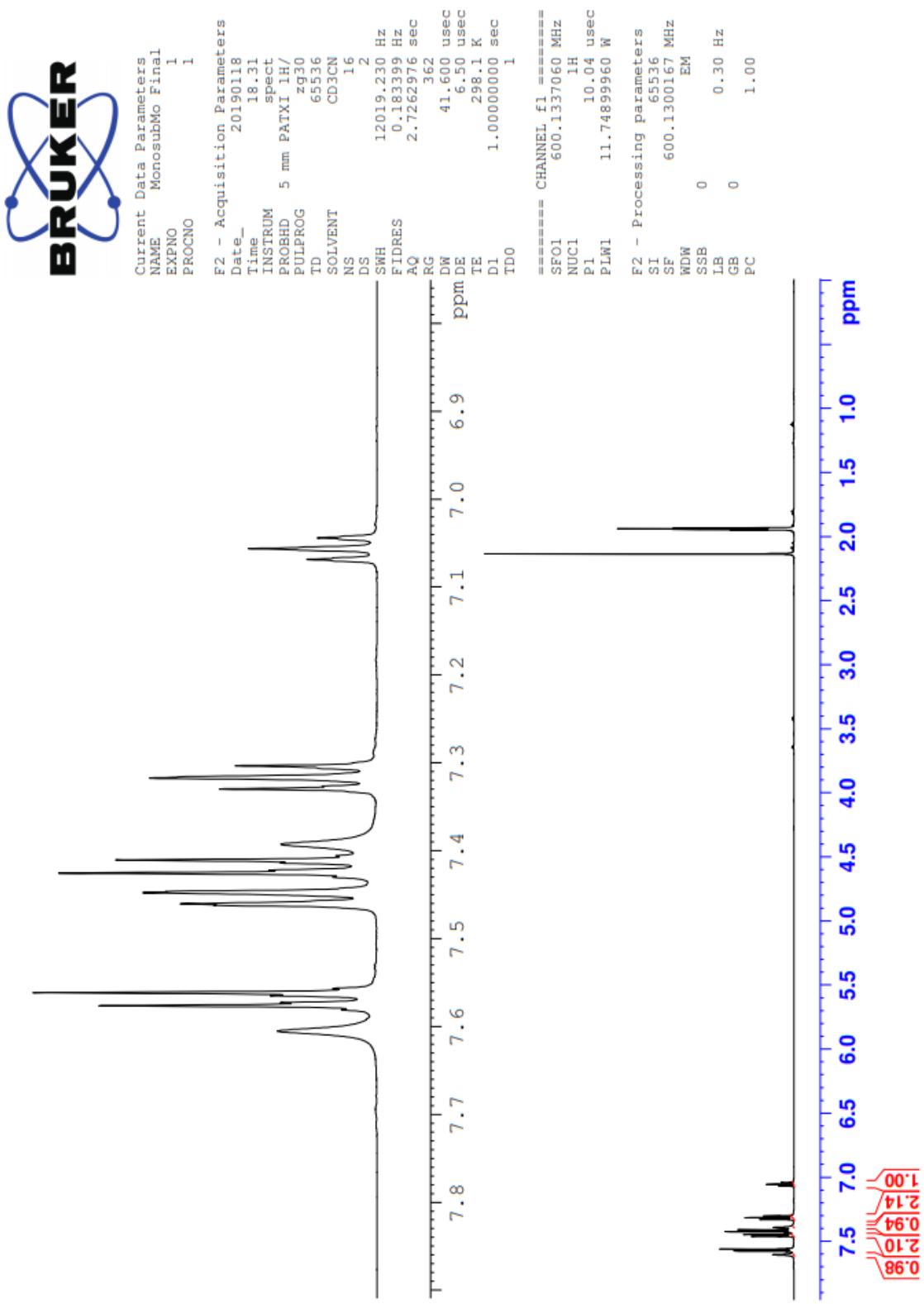
BRUKER
Current Data Parameters
NAME MonosubMo Final
EXPNO 1
PROCNO 1
F2 - Acquisition Parameters
Date_ 20190118
Time 18.31
INSTRUM spect
PROBHD 5 mm PATXI 1H/
PULPROG zg30
TD 65536
SOLVENT CD3CN
NS 16
DS 2
SWH 12019.230 Hz
FIDRES 0.183399 Hz
AQ 2.7262976 sec
RG 362
DW 41.600 usec
DE 6.50 usec
TE 298.1 K
D1 1.00000000 sec
TD0 1
======== CHANNEL f1 ========
SFO1 600.1337060 MHz
NUC1 1H
P1 10.04 usec
PLW1 11.74899960 W
F2 - Processing parameters
SI 65536
SF 600.1300167 MHz
WDW EM
SSB 0
LB 0.30 Hz
GB 0
PC 1.00
ppm
0.98
2.10
0.94
2.14
1.00

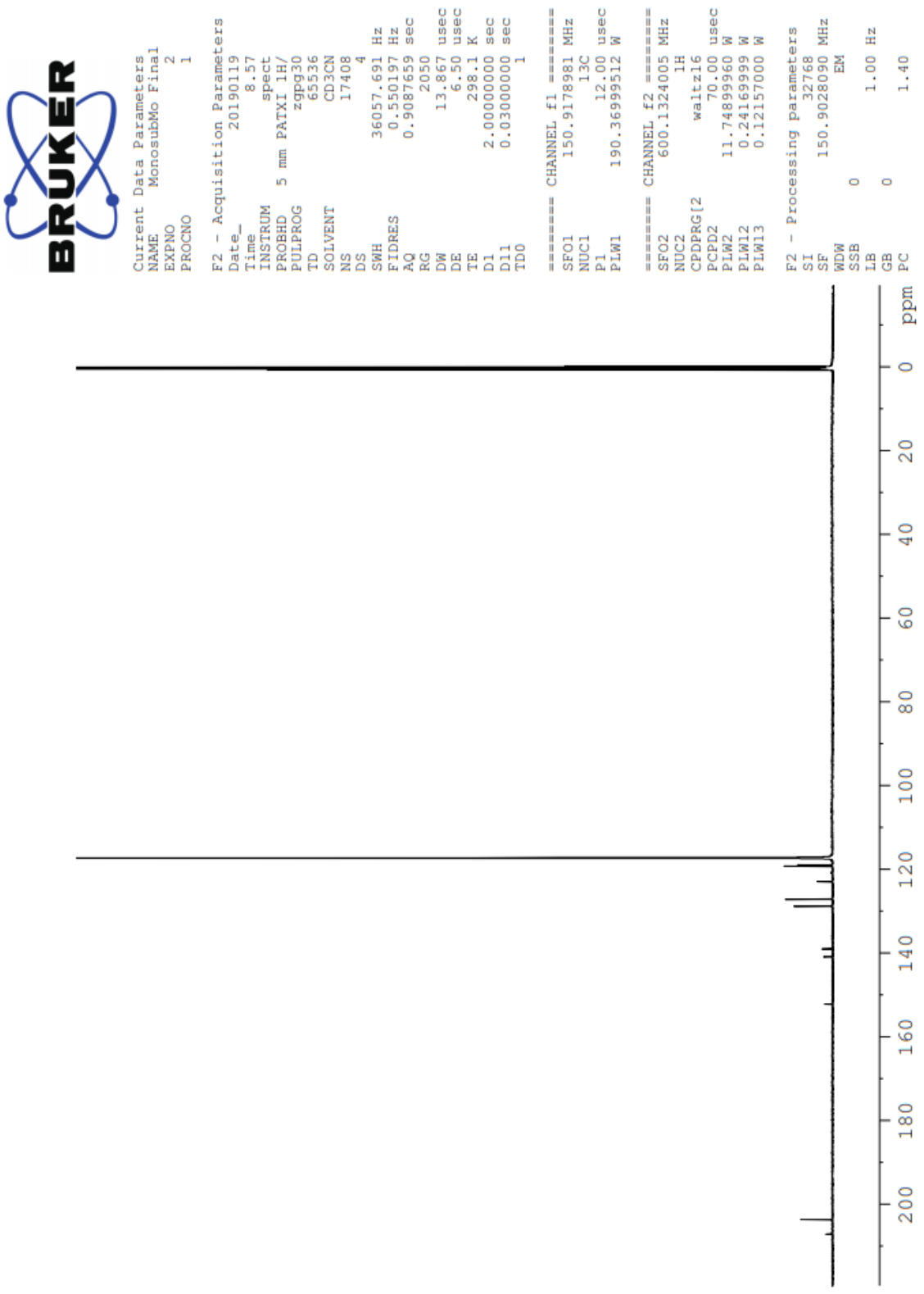
Current Data Parameters
NAME MonosubMo Final
EXPNO 2
PROCNO 1
F2 - Acquisition Parameters
Date_ 20190119
Time 8.57
INSTRUM spect
PROBHD 5 mm PATXI 1H/
PULPROG zgpg30
TD 65536
SOLVENT CD3CN
NS 17408
DS 4
SWH 36057.691 Hz
FIDRES 0.550197 Hz
AQ 0.9087659 sec
RG 2050
DW 13.867 usec
DE 6.50 usec
TE 298.1 K
D1 2.00000000 sec
D11 0.03000000 sec
TD0 1
======== CHANNEL f1 ========
SFO1 150.9178981 MHz
NUC1 13C
P1 12.00 usec
PLW1 190.36999512 W
======== CHANNEL f2 ========
SFO2 600.1324005 MHz
NUC2 1H
CPDPRG[2 waltz16
PCPD2 70.00 usec
PLW2 11.74899960 W
PLW12 0.24169999 W
PLW13 0.12157000 W
F2 - Processing parameters
SI 32768
SF 150.9028090 MHz
WDW EM
SSB 0
LB 1.00 Hz
GB 0
PC 1.40
200 180 160 140 120 100 80 60 40 20 0 ppm

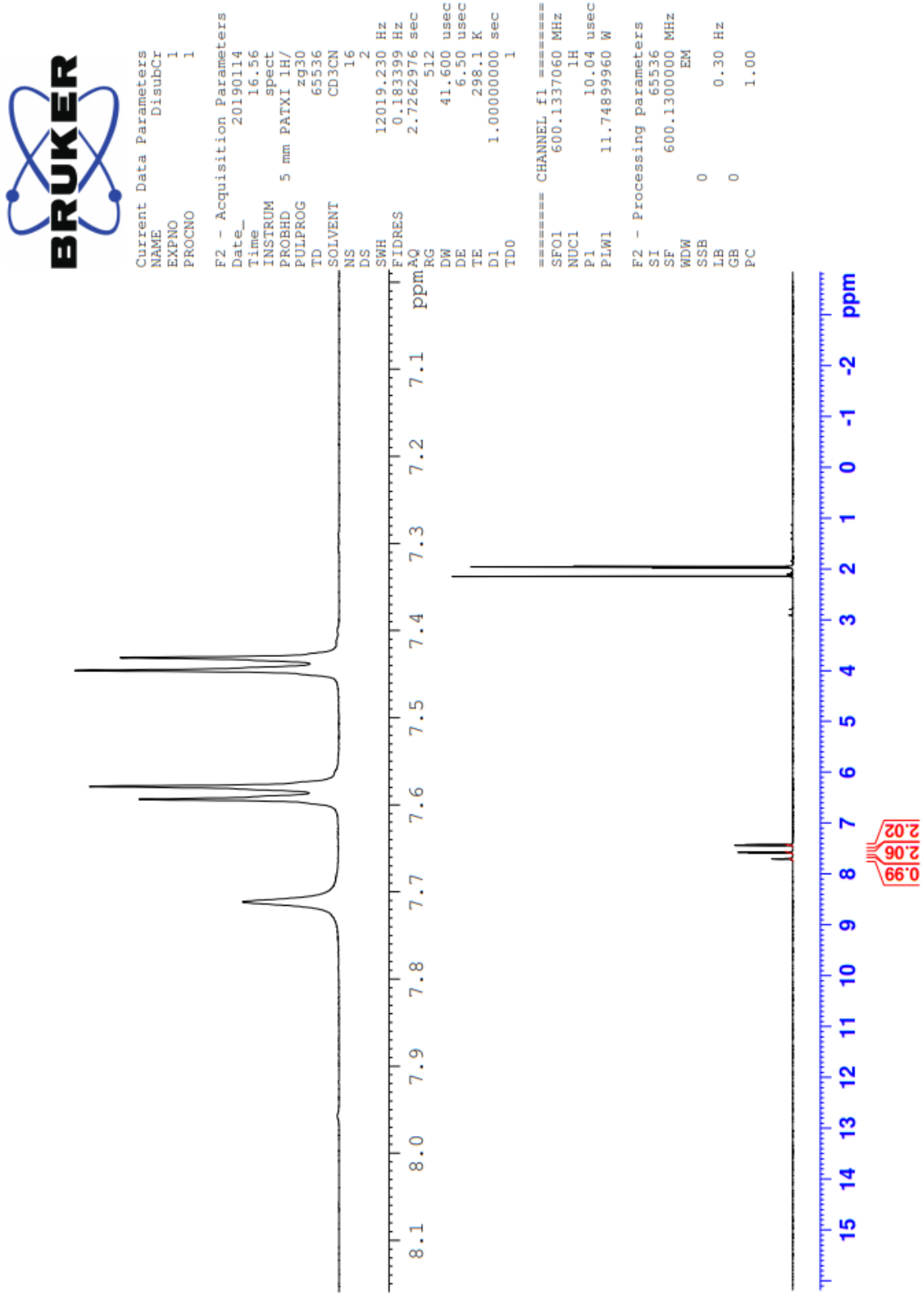
Current Data Parameters
NAME DisubCr
EXPNO 1
PROCNO 1
F2 - Acquisition Parameters
Date_ 20190114
Time 16.56
INSTRUM spect
PROBHD 5 mm PATXI 1H/
PULPROG zg30
TD 65536
SOLVENT CD3CN
NS 16
DS 2
SWH 12019.230 Hz
FIDRES 0.183399 Hz
AQ 2.7262976 sec
RG 512
DW 41.600 usec
DE 6.50 usec
TE 298.1 K
D1 1.00000000 sec
TD0 1
======== CHANNEL f1 ========
SFO1 600.1337060 MHz
NUC1 1H
P1 10.04 usec
PLW1 11.74899960 W
F2 - Processing parameters
SI 65536
SF 600.1300000 MHz
WDW EM
SSB 0
LB 0.30 Hz
GB 0
PC 1.00
ppm
0.99
2.06
2.02

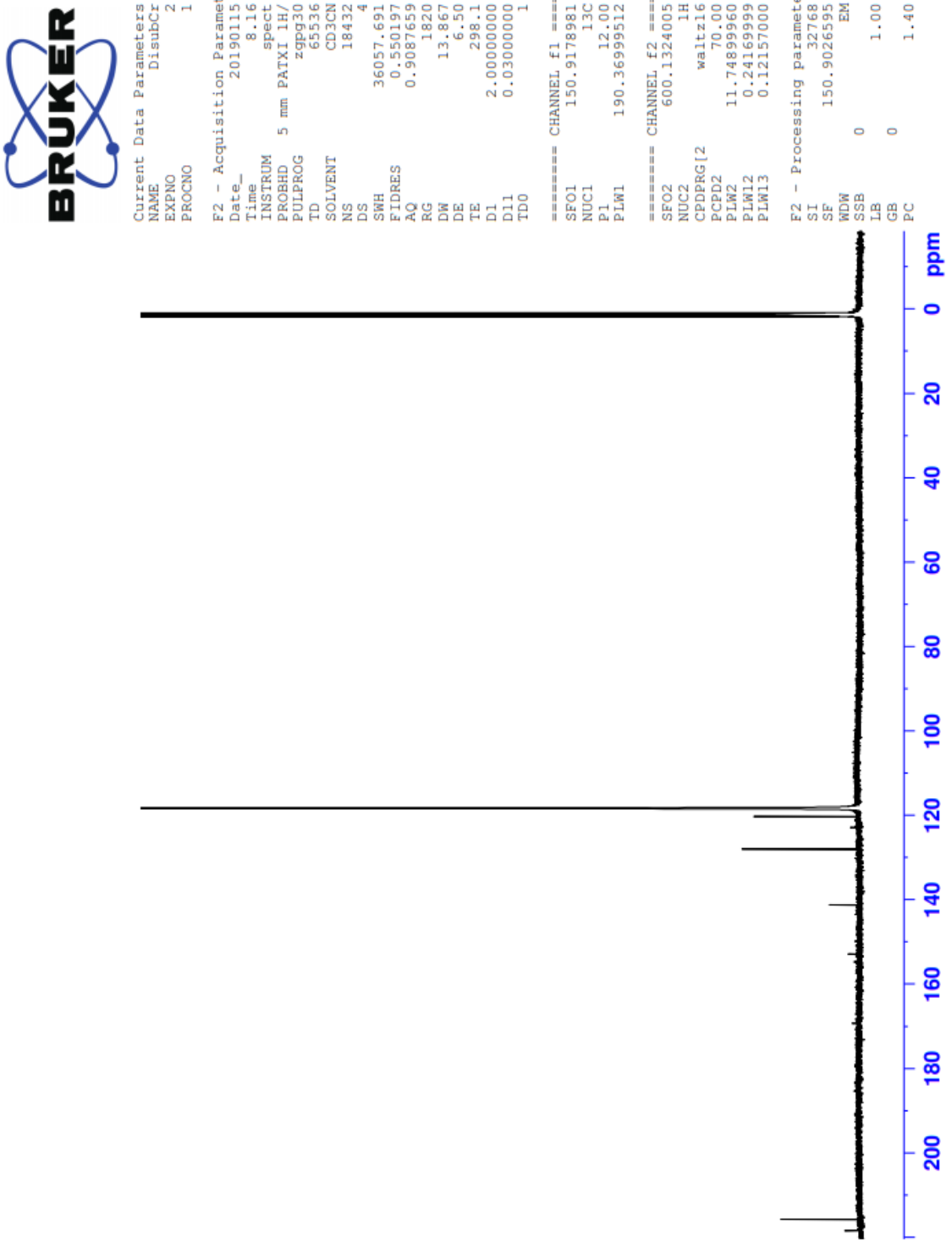
Current Data Parameters
NAME DisubCr
EXPNO 2
PROCNO 1
F2 - Acquisition Parameters
Date_ 20190115
Time 8.16
INSTRUM spect
PROBHD 5 mm PATXI 1H/
PULPROG zgpg30
TD 65536
SOLVENT CD3CN
NS 18432
DS 4
SWH 36057.691 Hz
FIDRES 0.550197 Hz
AQ 0.9087659 sec
RG 1820
DW 13.867 usec
DE 6.50 usec
TE 298.1 K
D1 2.00000000 sec
D11 0.03000000 sec
TD0 1
======== CHANNEL f1 ========
SFO1 150.9178981 MHz
NUC1 13C
P1 12.00 usec
PLW1 190.36999512 W
======== CHANNEL f2 ========
SFO2 600.1324005 MHz
NUC2 1H
CPDPRG[2 waltz16
PCPD2 70.00 usec
PLW2 11.74899960 W
PLW12 0.24169999 W
PLW13 0.12157000 W
F2 - Processing parameters
SI 32768
SF 150.9026595 MHz
WDW EM
SSB 0
LB 1.00 Hz
GB 0
PC 1.40
200
180
160
140
120
100
80
60
40
20
0
ppm

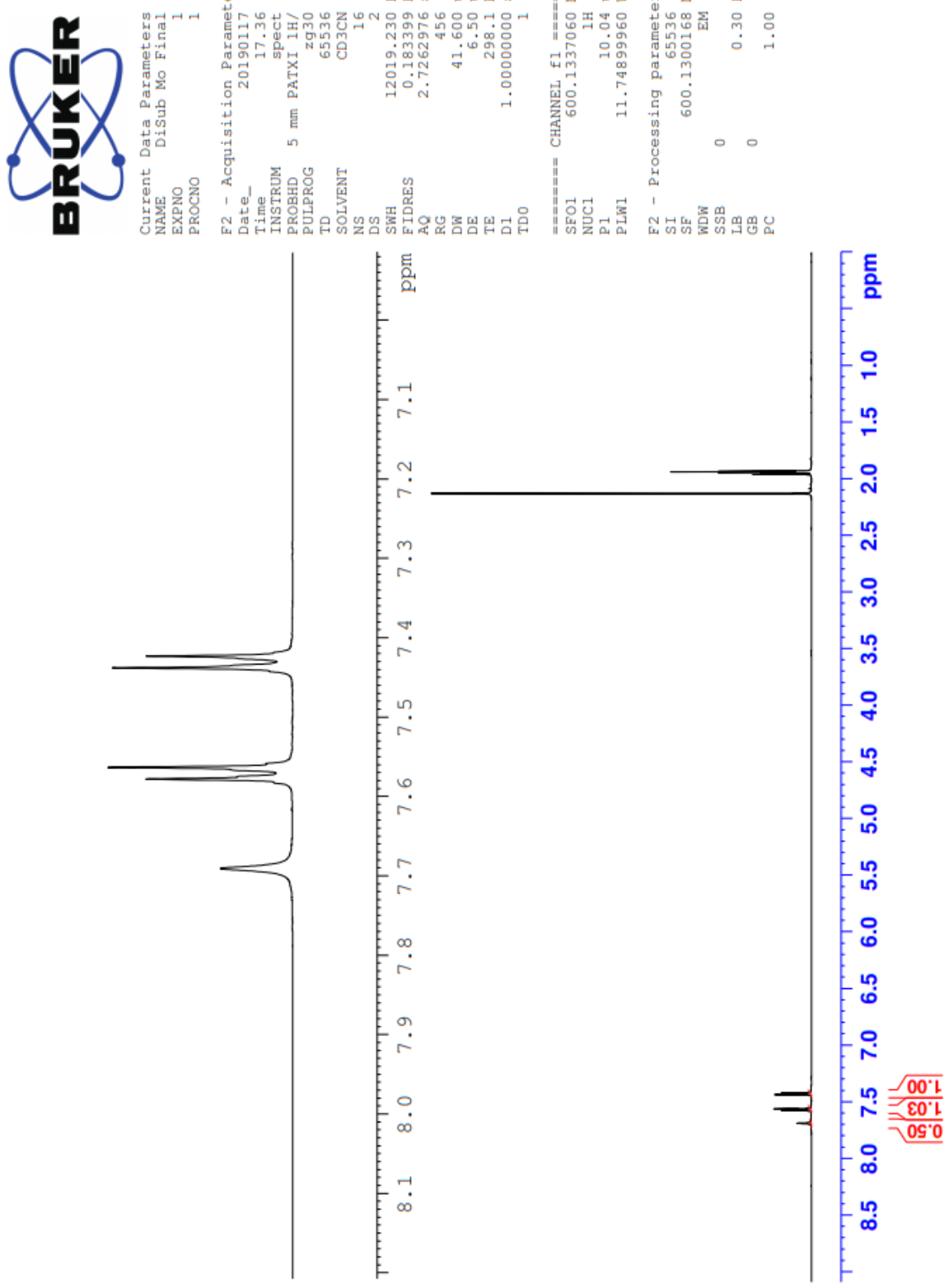
Current Data Parameters
NAME DiSub Mo Final
EXPNO 1
PROCNO 1
F2 - Acquisition Parameters
Date_ 20190117
Time 17.36
INSTRUM spect
PROBHD 5 mm PATXI 1H/
PULPROG zg30
TD 65536
SOLVENT CD3CN
NS 16
DS 2
SWH 12019.230 Hz
FIDRES 0.183399 Hz
AQ 2.7262976 sec
RG 456
DW 41.600 usec
DE 6.50 usec
TE 298.1 K
D1 1.00000000 sec
TD0 1
======== CHANNEL f1 ========
SFO1 600.1337060 MHz
NUC1 1H
P1 10.04 usec
PLW1 11.74899960 W
F2 - Processing parameters
SI 65536
SF 600.1300168 MHz
WDW EM
SSB 0
LB 0.30 Hz
GB 0
PC 1.00
ppm
0.50
1.03
1.00

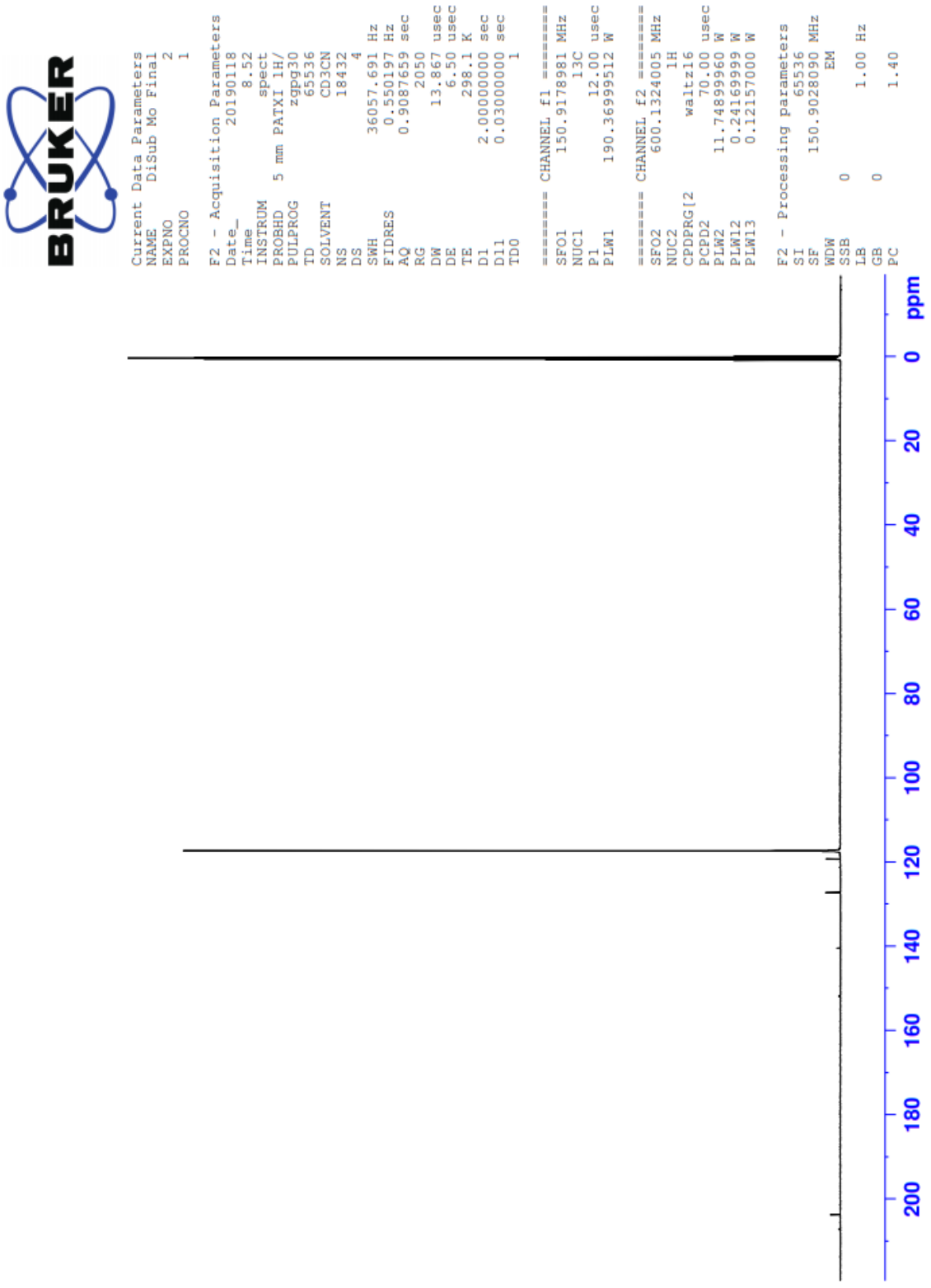
Current Data Parameters
NAME DiSub Mo Final
EXPNO 2
PROCNO 1
F2 - Acquisition Parameters
Date_ 20190118
Time 8.52
INSTRUM spect
PROBHD 5 mm PATXI 1H/
PULPROG zgpg30
TD 65536
SOLVENT CD3CN
NS 18432
DS 4
SWH 36057.691 Hz
FIDRES 0.550197 Hz
AQ 0.90876659 sec
RG 2050
DW 13.867 usec
DE 6.50 usec
TE 298.1 K
D1 2.00000000 sec
D11 0.03000000 sec
TD0 1
======== CHANNEL f1 ========
SFO1 150.9178981 MHz
NUC1 13C
P1 12.00 usec
PLW1 190.36999512 W
======== CHANNEL f2 ========
SFO2 600.1324005 MHz
NUC2 1H
CPDPRG[2 waltz16
PCPD2 70.00 usec
PLW2 11.74899960 W
PLW12 0.24169999 W
PLW13 0.12157000 W
F2 - Processing parameters
SI 65536
SF 150.9028090 MHz
WDW EM
SSB 0
LB 1.00 Hz
GB 0
PC 1.40
200
180
160
140
120
100
80
60
40
20
0
ppm

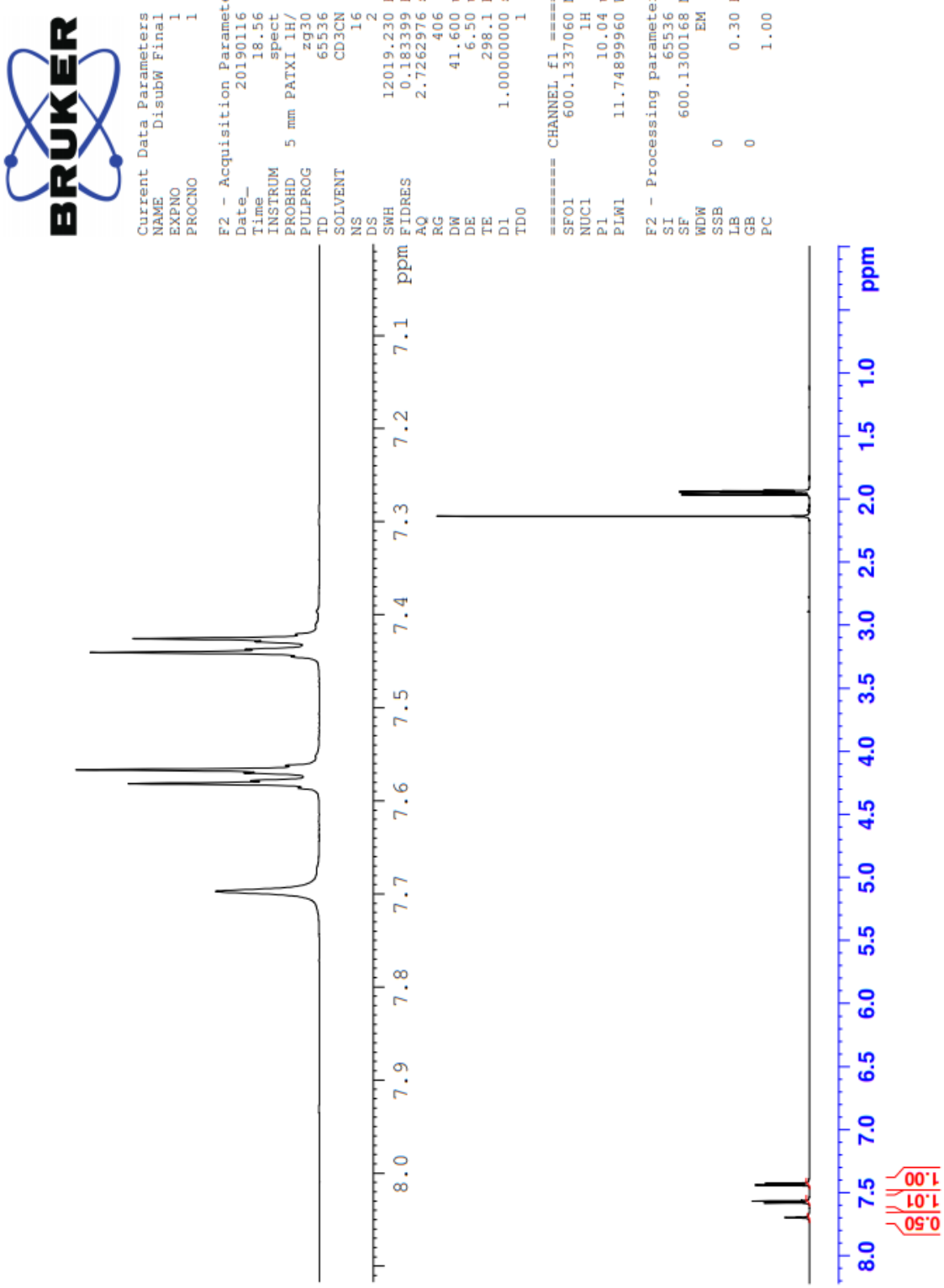
Current Data Parameters
NAME DisubW Final
EXPNO 1
PROCNO 1
F2 - Acquisition Parameters
Date_ 20190116
Time 18.56
INSTRUM spect
PROBHD 5 mm PATXI 1H/
PULPROG zg30
TD 65536
SOLVENT CD3CN
NS 16
DS 2
SWH 12019.230 Hz
FIDRES 0.183399 Hz
AQ 2.7262976 sec
RG 406
DW 41.600 usec
DE 6.50 usec
TE 298.1 K
D1 1.00000000 sec
TD0 1
======== CHANNEL f1 ========
SFO1 600.1337060 MHz
NUC1 1H
P1 10.04 usec
PLW1 11.74899960 W
F2 - Processing parameters
SI 65536
SF 600.1300168 MHz
WDW EM
SSB 0
LB 0.30 Hz
GB 0
PC 1.00
ppm
0.50
1.01
1.00

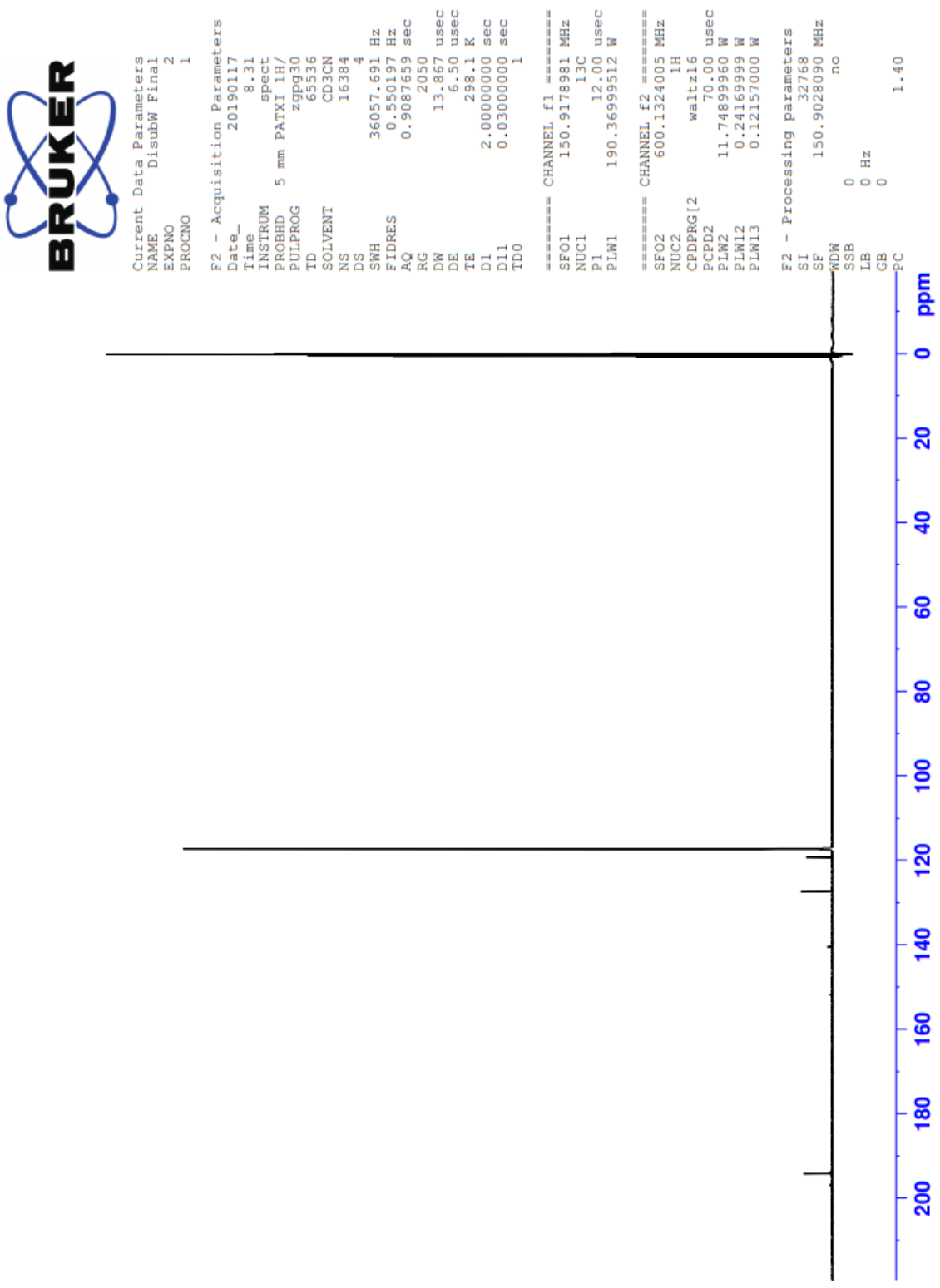
Current Data Parameters
NAME Disubw Final
EXPNO 2
PROCNO 1
F2 - Acquisition Parameters
Date_ 20190117
Time 8.31
INSTRUM spect
PROBHD 5 mm PATXI 1H/
PULPROG zgpg30
TD 65536
SOLVENT CD3CN
NS 16384
DS 4
SWH 36057.691 Hz
FIDRES 0.550197 Hz
AQ 0.9087659 sec
RG 2050
DW 13.867 usec
DE 6.50 usec
TE 298.1 K
D1 2.00000000 sec
D11 0.03000000 sec
TD0 1
======== CHANNEL f1 ========
SFO1 150.9178981 MHz
NUC1 13C
P1 12.00 usec
PLW1 190.36999512 W
======== CHANNEL f2 ========
SFO2 600.1324005 MHz
NUC2 1H
CPDPRG[2 waltz16
PCPD2 70.00 usec
PLW2 11.74899960 W
PLW12 0.24169999 W
PLW13 0.12157000 W
F2 - Processing parameters
SI 32768
SF 150.9028090 MHz
WDW no
SSB 0
LB 0 Hz
GB 0
PC 1.40
200
180
160
140
120
100
80
60
40
20
0
ppm

IR DATA